Archaeological and Anthropological Sciences (2020) 12: 88
https://doi.org/10.1007/s12520-020-01035-z

ORIGINAL PAPER

Geoarchaeological evidence of Ostia's river harbour operating until the fourth century AD

A. Vött[1] · T. Willershäuser[1] · H. Hadler[1] · L. Obrocki[1] · P. Fischer[1] · M. Heinzelmann[2]

Received: 6 December 2019 / Accepted: 17 February 2020 / Published online: 17 March 2020

Abstract

Ancient Ostia at the mouth of the River Tiber into the Tyrrhenian Sea was largely significant for the economic supply of Rome. Ostia itself experienced an extraordinary period of prosperity in the second century AD. Starting in AD 42, a first new harbour at Portus was built by Emperor Claudius close to Ostia. It reached its full functionality under Emperor Trajan in the early second century AD, only. At Ostia itself, previous archaeological and geoarchaeological studies have brought to light a lagoon-type harbour at the western fringe of the city operating between the fourth and the second century BC in an artificially excavated harbour basin. From the second century BC onwards, a considerably smaller and shallower part of this western harbour basin was still in function as a fluvial harbour. So far, it was unclear whether Ostia's western harbour was still in use when the harbour at Portus was set into function in the first to second century AD, or if the latter partially replaced Ostia's harbour infrastructure. According to archaeological evidence, Ostia's navalia-temple-complex, the main building at the eastern fringe of the western river harbour basin, was built in the second quarter of the first century AD. Was this prestigious harbour building erected although the associated harbour seemed to have been already given up before? We conducted detailed geoarchaeological investigations at the immediate western front of the navalia-temple complex. Results were compared with archaeological data obtained from excavations carried out in 2000/2001. A multi-proxy approach was used to reconstruct the history and evolution of the harbour. It was possible to identify subsurface structures and evaluate the local stratigraphy. Vibracoring brought to light a more than 1 m thick section of an *opus reticulatum* wall with parts of the original *opus latericium* on top. Such walls originally separated vaulted shipshed chambers of the navalia-temple complex at Ostia, which in turn formed the substructure of a temple complex located above it. Another core revealed the sedimentary infill of a former chamber of the building. Based on radiocarbon dating, the navalia was in use between the first and the fourth centuries AD with a water depth of maximum ca. 1.2 m at the immediate western front. This is in agreement with the date of construction of the navalia-temple complex in the second quarter of the first century AD. The relative sea level at that time was around 0.64 m below the present sea level. The harbour and the navalia were obviously accessible only for flat-keeled lighters and cargo boats. Larger cargo ships were either unloaded along the riverbank to the north of ancient Ostia (Hadler et al. 2019) or moored offshore, their freight being reloaded to smaller lighters. Chronostratigraphic data further show that the navalia-temple complex was in use until the second half of the fourth century AD. It was not before AD 355–363 or shortly afterwards, that the harbour site was abandoned. Ostia's western river harbour was neither abandoned nor completely silted up before the harbour at Portus was established as previously assumed by other authors. Actually, the western front of the navalia-temple complex was hit by an extreme wave event, leaving a sand layer approx. 0.5 m thick, at or shortly after AD 355–363 which led to the final abandonment of Ostia's western river harbour. This event is interpreted as a tsunami that may have hit the wider coastal region.

Keywords Ancient Ostia · Harbour · Navalia-temple-complex · River Tiber · Tsunami

✉ A. Vött
voett@uni-mainz.de

[1] Institute of Geography, Johannes Gutenberg-Universität Mainz, Johann-Joachim-Becher-Weg 21, 55099 Mainz, Germany

[2] Institute of Archaeology, Universität zu Köln, Albertus-Magnus-Platz, 50923 Köln, Germany

Introduction and geoarchaeological key question concerning Ostia's river harbour

Ancient Ostia at the mouth of the River Tiber into the Tyrrhenian Sea was largely significant for the economic supply of nearby Rome lying ca. 25 km further upstream (Fig. 1). Ostia was founded in the second half of the fourth century BC as a Roman colony to guarantee the delivery of trade and goods from all over the Mediterranean Sea to the Tiber River mouth. However, various indications point to the fact that the site of the later city had already been the site of first settlement and trading activities since the sixth century BC. So to say, ancient Ostia was the gateway to Rome over centuries. For this reason, the question where ancient Ostia's harbour capacities were situated, is of crucial importance to a better understanding of Ostia's and Rome's history. After a rather slow development during the late Republican and early Imperial period, Ostia experienced an unparalleled urban boom in the second century AD, based on a sharp increase in commercial activities. Almost the entire city was rebuilt in a very short time, which now includes many warehouses and granaries. However, the economic situation stagnated during the third century AD (Heinzelmann 2010). Starting in 42 AD under the Roman Emperor Claudius, the new harbour Portus was built ca. 3.5 km to the northwest of ancient Ostia, but the harbour obtained its full functionality only under Emperor Trajan in the early second century AD by large rebuilding measures (Keay et al. 2005: 270–290).

In Ostia, the river bank of the Tiber has always served as a transshipment zone (Hadler et al. 2019), but the limited space and regular low water levels during the summer limited its functionality. In addition, already in the nineteenth century, another possible harbour was assumed in a topographical depression between the Tor Boacciana and the Palazzo Imperiale on the left river bank of the River Tiber near its original mouth. First archaeological evidence was presented within the framework of geophysical and archaeological studies in the late 1990s and early 2000s by Heinzelmann (Heinzelmann 1998, 2001, 2010) and Heinzelmann and Martin (2002). Based on their studies, an artificial harbour basin was localized, for the first time. Moreover, on its eastern side, a large building was identified, the remains of which were interpreted as a navalia-temple complex (Heinzelmann and Martin 2002; Martin et al. 2002). It consisted of a platform, on which stood

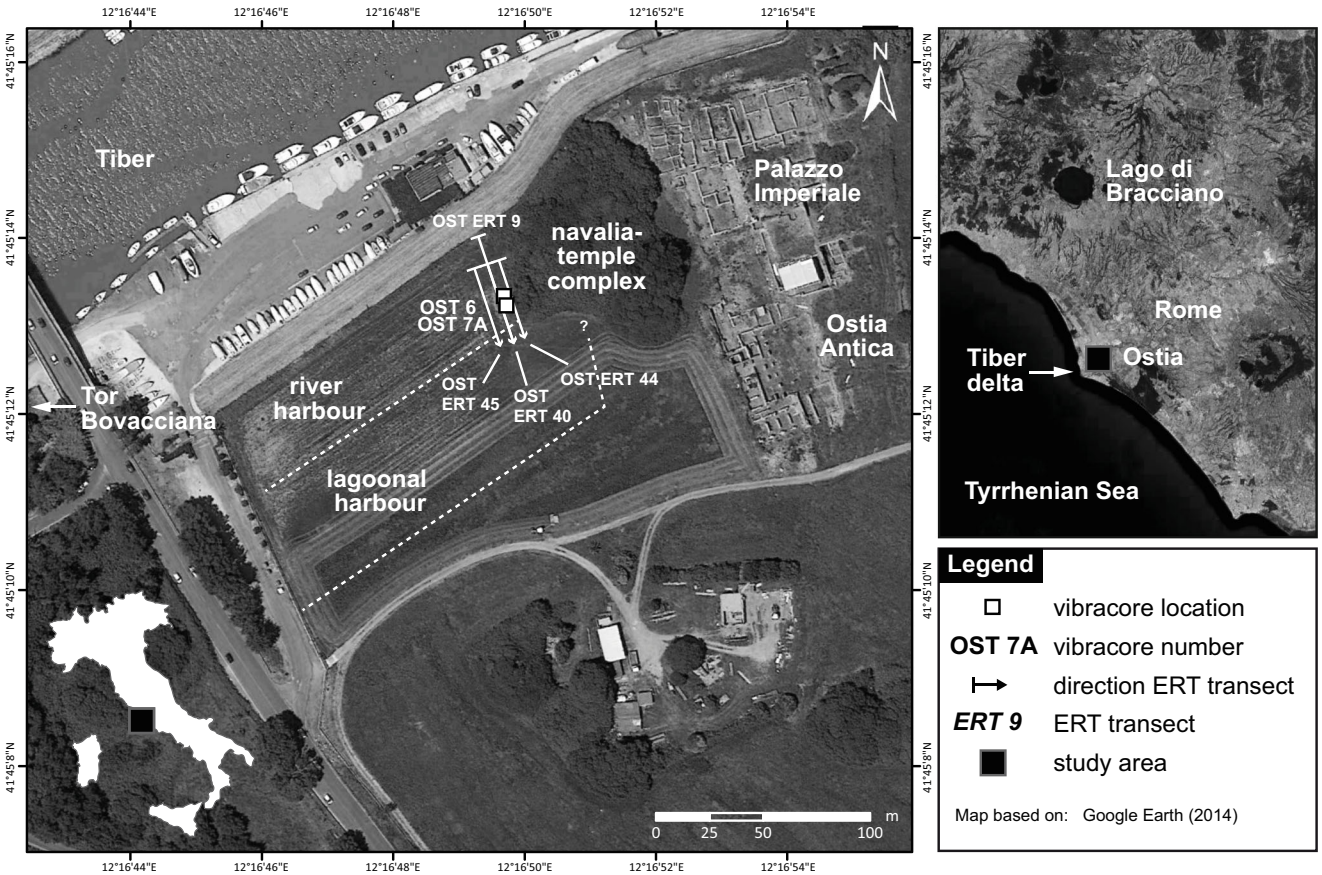

Fig. 1 Topographic overview of the western river harbour of ancient Ostia to the south of the River Tiber. The basin of a lagoonal harbour was excavated from older marine sands. This harbour was in function between the fourth and second century BC (Hadler et al. 2015; Vött et al. 2015). The younger river harbour occupied only parts of the elder basin. It was associated with a prestigious navalia-temple complex at its northeastern fringe. Geoarchaeological studies were carried out in the immediate front of the building to clarify how long the harbour was used

a large temple with surrounding porticoes, facing the mouth of the Tiber. The substructure of the platform consisted of numerous long vaulted chambers which opened towards the Tiber and the harbour basin to the west with flat ramps made of *opus caementicium* (Heinzelmann 2020, see Section 2). These vaulted chambers were considered as possible shipsheds (navalia), whereby their size (max. 35 m long, 5 m wide, 5 m high) have only allowed the storage of smaller ships, e.g. river warships.

During the early 2010s, first geoarchaeological investigations in the harbour basin brought to light geological evidence of associated harbour deposits (Goiran 2012; Goiran et al. 2012, 2014). Further systematic geophysical and sedimentological studies allowed to discriminate between two different harbour generations: a first lagoonal harbour, in use between the fourth and at least the second century BC, and a subsequent river harbour. Geophysical and stratigraphic data prove that the harbour basin associated with the lagoonal harbour was excavated from older fluvio-deltaic and marine sand deposits (Vött et al. 2015) down to more than 5.5 m below present sea level (b.s.l.). Considering a local relative sea level stand during Roman times of at least 0.8 m lower than today as found around Portus by Goiran et al. (2010), the lagoonal harbour basin was at least 4.7 m deep and thus apt for even large cargo ships (Goiran et al. 2014). From the second century BC onwards, the considerably smaller and shallower western river harbour was in function.

So far, there is a vivid discussion on how long this western fluvial harbour basin was in use and how the relation with the nearby Portus harbour has to be evaluated. While Hadler et al. (2015) and Vött et al. (2015) are convinced that Ostia's western river harbour was still in use when the harbour at Portus was set into function, Goiran et al. (2014) and, at the latest, Salomon et al. (2018) argue that water depth was too shallow and the harbour was almost completely silted at the end of the 1st quarter of the first century AD, namely, some 2 decades before construction works for Portus have begun. Based on archaeological evidence, however, the large and impressive main building of the river harbour, the navalia-temple-complex located at the eastern fringe of the harbour basin, was built in the second quarter of the first century AD (Heinzelmann and Martin 2002). The main question thus is: was this prestigious harbour building erected after the associated harbour had been given up a few decades before?

The main objectives of the study presented in this paper are (i) to investigate the relationship between harbour deposits and the navalia-temple-complex at Ostia's western river harbour by means of geoarchaeological methods, (ii) to compare (geo-)archaeological stratigraphic information with relative sea level data for the time when the harbour was in function, (iii) to unravel the history of the river harbour as documented by harbour sediments and archaeological data, and (iv) to clarify how long the harbour was in use and which factors led to its abandonment.

The navalia-temple complex at Ostia

Excavation history and general observations

An in-depth-description of the navalia-temple complex is given by Heinzelmann (2020). The complex is located at the eastern fringe of the harbour basin and measures ca. 67 m × 78.5 m (Fig. 2). It consisted of a large terrace built on top of tunnel vault-type substruction chambers. These chambers were open towards the four sides of the complex and, therefore, arranged orthogonal to each other. The northern and southern chambers are the longest (ca. 35 m) whereas the eastern chambers are the shortest and irregular in length. Along three sides, the terrace was framed by a *porticus*. In its centre, there was a temple facing towards the Tiber River mouth. The western chambers of the substruction terrace directly opened towards the harbour basin with flat ramps (Heinzelmann 2020). For this reason, they were most probably used as shipsheds (navalia) or may at least have intentionally produced the impression as if they were.

The northeastern part of the complex was systematically excavated by C.L. Visconti in the midst of the nineteenth century but remained almost completely undocumented (Visconti 1857). Later, the northwestern part of the ruin was completely covered by the modern dam of the Tiber River and a landing place for sport boats without any further documentation (Fig. 2). Apart from cleansing and topographical survey of the superficial remains, two sondages were carried out within the frame of archaeological investigations in 2000 and 2001 (Heinzelmann 2020): sondage 21 covers the southwestern edge of the complex with its front towards the harbour basin including the corresponding substruction chambers, and sondage 33 was made to investigate the fundaments of the temple. In 2013, ground penetrating radar (GPR) measurements were conducted in the area of the landing site for sport boats but no evidence was found that architectural remains still exist underneath the concrete platform.

Visconti (1857) was the first to identify the archaeological remains at the eastern fringe of the harbour basin with shipsheds (navalia). He argued with the similarity of the architectural remains compared with a mosaic from a grave at the Porta Romana where a vault-type substruction was shown in conjunction with ships. Moreover, his interpretation was based on the former proximity to the sea and the River Tiber. This interpretation was also supported by Lanciani (1868).

The complex is first described in detail by Paschetto (1912). He interpreted the northern substruction chambers to be directly open towards the River Tiber and

Fig. 2 Archaeological plan of the navalia-temple complex adapted from Heinzelmann (2020). The substruction of the temple terrace was made out of vaulted chambers arranged in a rectangular structure. Sondage 21 was excavated at the southwestern front of the building and documented that the western chambers were used as navalia (Heinzelmann and Martin 2002). Geoarchaeological studies were conducted in the immediate front of the western chambers between the southern fringe of the river harbour basin and the present-day Tiber river dam

used both as shelter and as dockyard for river boats. According to Paschetto (1912), the upper part of the vaults as well as the space in between neighbouring vaults consisted of a hard layer ("calcestruzzo") as a founding base for the terrace on top, followed by a sequence of *opus spicatum* and *opus caementitium*. In contrast, the model of Ostia created by Gismondi depicts the architectural remains as a warehouse complex (Calza et al. 1953). Meiggs (1973) doubted that the chambers were used as shipsheds assuming that the vaulted chambers were not long enough and their openings too narrow to be used by ships.

At the eastern side of the complex, six pillars made of tuff are still preserved in a distance of ca. 5.60 m, leaving a clear diameter of ca. 4.20–4.45 m in between each other (Heinzelmann 2020). However, basal tuff ashlars founded on a travertine block are still unearthed, so that the original height of the construction remains unknown. Altogether, Heinzelmann (2020) suggests maximum 15 vaulted chambers for this eastern side. The cusp of the vaults seems to correspond well with the height of the vaulted chambers found along the northern front of the complex. The eastern chambers were presumably used as workshops and shops (*tabernae*). In front of the vaulted chambers, there was a *porticus* out of *opus caementitium* pillars with an *opus latericium* face out of red bricks. Heinzelmann (2020) suggests that these pillars were built in the second century AD.

The vaulted chambers facing towards the north (Fig. 3) were already described by Paschetto (1912) and re-examined by Heinzelmann (2020). However, the northern ends of the chamber walls – still visible a century ago – nowadays disappear under the modern Tiber River dam (Fig. 2). The total length of each of the four vaulted chambers observed by Heinzelmann (2020) must have reached ca. 35 m (today: 20 m). The walls in between are ca. 0.65 cm thick and are made out of a regular *opus reticulatum* covered by a ca. 0.28 cm thick zone of *opus latericium* out of six brick layers (Fig. 3a–c). Their foundations are not visible. The upper room closure consists of a barrel vault made of *opus caementicium* with added fragments of tuffo and reticulate stones. The *caementicium* vault is completely covered by a layer of hydraulic mortar showing that the temple terrace above it was an open-air construction. On top of the hydraulic mortar, Heinzelmann (2020) found another zone of levelling made of *opus caementicium* covered by a floor out of *opus spicatum*.

Remains of vaulted chambers, partly intact, partly collapsed, were found along every one of the four sides of the navalia-temple-complex. The vaulted chambers at the southern side show the same width as those observed along the northern side of the complex (Fig. 2).

Fig. 3 (a–c) Photos of the preserved northern chamber N3 (see Fig. 2) of the navalia-temple complex at ancient Ostia. The vaulted ceiling out of *opus caementicium* can be easily discerned, also the *opus reticulatum* wall that originally separated chamber *N*3 from chamber *N*2 (not preserved). Detail photo in Fig. 3c shows construction details of this separating wall. (d–f) Geophysical prospection using ERT and vibracoring were carried out in the immediate western front of the navalia-temple complex at ancient Ostia in order to clarify the relation between the building and the harbour basin. Photos: A. Vött, 2013

Results of archaeological excavations in 2000 and 2001

The results of the archaeological excavations conducted in Ostia's western river harbour area in 2000 and 2001 are presented by Heinzelmann (2020). Two sondages were carried out, namely, sondage 21 and sondage 33 (Fig. 2). In the following, the most important archaeological findings are summarized based on Heinzelmann (2020).

Sondage 21: southwestern corner and harbour front of the navalia terrace

The maximum depth of sondage 21 was limited by the high groundwater level during excavation activities in 2000. In general, no recent interference was found but the ancient remains were covered by thick sediment layers. Remains of buildings found in sondage 21 were partly disturbed by spoliation and effects of post-ancient floods.

Three large ashlars were found, forming a joint front towards the harbour basin (Fig. 2). The lower edges of the ashlars could not be unearthed because of the high groundwater level. The ashlars probably represent remains of pillar structures that originally bore chamber vaults in analogy to the findings from the eastern side of the complex. The southern ashlar marks the southwestern corner of the entire building as shown by an adjoining apsidal-type building. The east-west trending walls belong to the same construction phase as the ashlars and consist of a rough *opus reticulatum* with the corners reinforced by bricks, all sections cemented by a hydraulic mortar. The structure of the wall is completely identical with the vaulted chambers on the northern front of the navalia-temple complex (Figs. 3a, c). Sondage 21 thus revealed evidence of three parallel chambers, the southern one being 3.50 m wide, whereas the two others showing a width of 5.0 m each (Figs. 2, 3, 4). The chambers' floor was made out of massive *opus caementicium* with hydraulic mortar showing an inclination of ca. 5° and rising from west to east. Moreover, sea level-related outwash marks were found at the western faces of the basal ashlars documenting the impact of breaking waves and tidal changes. These features also document that the chambers must have been open towards the harbour basin, the *opus caementicium* floors reaching the former water level or lying beneath it.

In general, shipsheds were not used for large cargo ships with heavy planking, but rather for flat-keeled warships, fishing boats, ferry boats, or lighters for shelter or to allow repair measures during the winter season (Heinzelmann 2020). Usually, ships were towed in with their stern first and stored on wooden rolls or planks. In contrast to ancient Greek contexts, shipsheds have been rarely found in Roman sea or river harbours. However, ancient accounts do also attest the existence of navalia, for example for Rome and Ostia (Blackman et al. 2014). At Ostia, the chambers opening to the west are characterised by comparatively small dimensions. Heinzelmann (2020) suggests that they were used for small, short river warships similar to the Lusoria-type rowing boats (Ferkel et al. 2004). Also, one might think of private rowing and towing boats stored in the western chambers. The northern chambers also seem to have been used as shipsheds although they are arranged perpendicular to the Tiber River. However, similar examples of navalia along rivers show that this constellation was not a problem for the ship crews at that time (Coarelli 1997; Heinzelmann 2020).

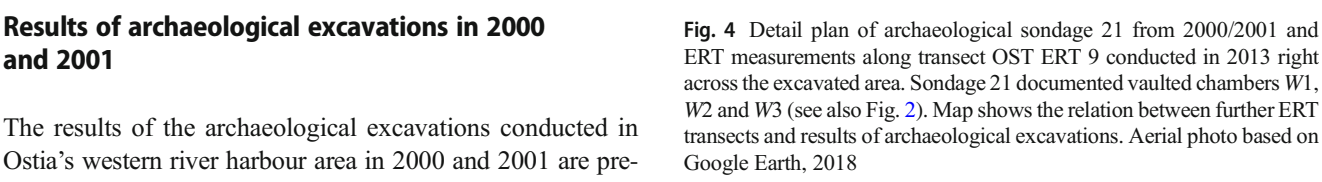

Fig. 4 Detail plan of archaeological sondage 21 from 2000/2001 and ERT measurements along transect OST ERT 9 conducted in 2013 right across the excavated area. Sondage 21 documented vaulted chambers *W1*, *W2* and *W3* (see also Fig. 2). Map shows the relation between further ERT transects and results of archaeological excavations. Aerial photo based on Google Earth, 2018

The general dimensions of the chambers are identical with chambers found on the southern, eastern, and northern sides of the complex (Fig. 3). The fact that chambers revealed by sondage 21 were also covered by vaults is proven by *opus caementicium* findings, fragments of the hydraulic mortar cover, and by parts of the *opus spicatum* floor. Sondage 21 thus provides evidence of the western front of the complex facing the harbour basin. A sediment layer found adjoining one of the basal ashlars allows to fix the early first century AD as a rough *terminus post quem* for the construction of the complex. In addition, results of sondage 33 allow to narrow the construction time to the second quarter of the first century AD (see below). Shortly above the ashlar level, a new surface horizon in the apsidal building was formed in the midst of the first century AD as shown by several embedded coins dating to the reigns of Claudius. This layer represents the first phase of intense use of the entire navalia-temple complex. Further evidence of the apsidal building was produced by GPR measurements in 2013 showing that the apsis is ca. 20 m wide and ca. 9 m deep. Later, an artificial levelling with a new floor was brought into the apsidal room. This floor was dated by a coin to the third quarter of the fourth century AD. This represents the latest use of this part of the building before its ceiling collapsed. Both the building and the harbour basin were subsequently filled by a thick layer of sand, ceramic, and architectural remains. Then, massive spoliation took place before the remains of the ruin and the harbour area were repeatedly flooded and covered by sand layers. Based on magnetite contents originating from the upper course of the Tiber River and sediment colours similar to the colours of recent beach deposits, Heinzelmann (2020) suggests that the sand layers attest to river floods and to extreme flooding events from the seaside, respectively. After these flooding events, the remaining walls collapsed completely. Later, the site was buried underneath fine-grained loamy deposits that

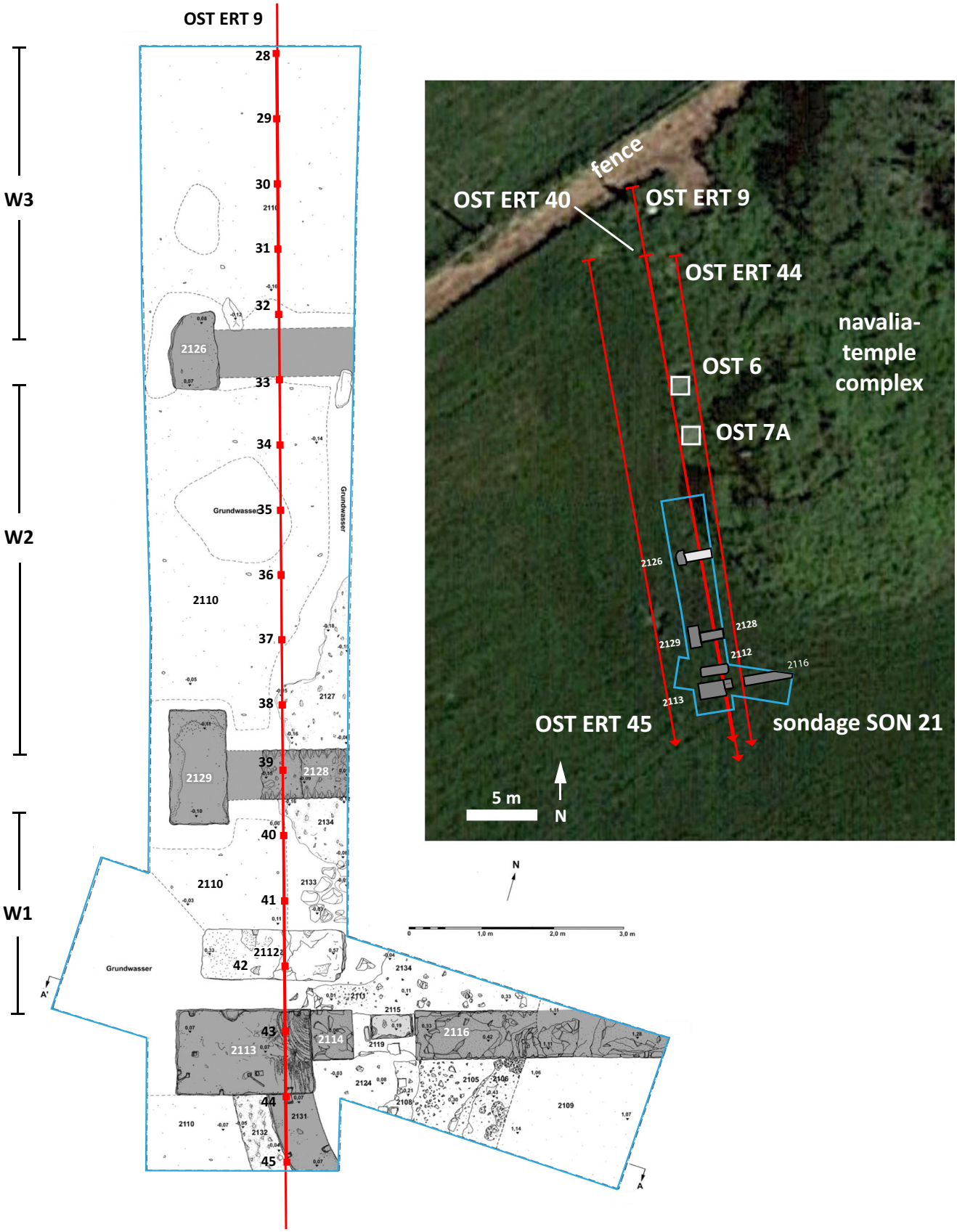
OST ERT 9
W3
W2
W1
28
29
30
31
32
33
34
35
36
37
38
39
40
41
42
43
44
45
2126
2110
2127
2129
2128
2134
2133
2112
2115
2116
2113
2114
2119
2124
2105
2106
2108
2109
2131
2132
Grundwasser
A'
A
0
1,0 m
2,0 m
3,0 m
N
fence
OST ERT 40
OST ERT 9
OST ERT 44
navalia-
temple
complex
OST 6
OST 7A
2126
2128
2129
2112
2116
2113
OST ERT 45
sondage SON 21
5 m
N

seem to have their origin in the River Tiber floods (Heinzelmann 2020).

Sondage 33: harbour temple

Sondage 33 was realized in the centre of the navalia-temple complex and brought to light the massive foundation walls of a large temple podium (ca. 19.5 m × 9.5 m) with its façade towards the Tiber River mouth (Fig. 2). While the foundations consisted of *opus caementicium* covered by *opus reticulatum*, numerous fragments of large building blocks and columns show that the upper structure of the temple was constructed entirely of Luni marble. The floor level of the temple's cella was located ca. 2 m above the *opus spicatum* floor of the navalia terrace. A pottery fragment embedded in mortar provides the 1st quarter of the first century AD as *terminus post quem* for the building. Moreover, a column base encountered is identical with the bases of the Roma and Augustus temple at Ostia's forum dated to the late Augustan or Tiberian period. Both findings support that the temple was built in the second quarter of the first century AD, while the first phase of intense use of the complex was dated – based on sondage 21 – to the midst of the first century AD (Heinzelmann 2020).

Heinzelmann (2020) reconstructs the total height of the temple to be 18 m plus another 5 m for the underlying terrace. The apex was thus located some 23 m above the water level at that time so that the temple represented a large, white landmark for ships approaching the Tiber River mouth.

Later, a new floor was made within the course of restoration works. These were dated to the time after AD 211 as evidenced by two embedded coins (Heinzelmann 2020). In later times, spoliation took place and the building was severely damaged due to the collapse of the underlying vaulted chambers. During modern times, local strata were strongly mixed and depressions filled up with soil and sediments.

Methods

Geoarchaeological studies at the navalia-temple complex were conducted within the framework of the Priority Program 1630 "Harbours from the Roman Period to the Middle Ages" funded by the German Research Foundation 2012–2018 (DFG SPP 1630, HE 3680/6–1, VO 938/10–1). Field work comprised detailed geophysical investigation of the river harbour area at ancient Ostia using a variety of different methods. Amongst others, systematic electrical resistivity tomography (ERT), seismic and ground penetrating radar (GPR) studies were carried out. These studies were the base to identify the dimensions and depth of the artificially excavated harbour basin associated with the lagoonal harbour that existed between the fourth and second century BC (Hadler et al. 2015; Vött et al. 2015; Wunderlich et al. 2018).

In this paper, we present new ERT data that was collected along several transects parallel to the western front of the navalia-temple-complex. ERT transects OST ERT 9 and OST ERT 40 were arranged in a way that they covered the study area of archaeological sondage 21 (Fig. 4). ERT measurements were carried out by means of a multi-electrode geoelectrical unit (type Syscal R1 plus Switch 48, Iris Instruments) using a Wenner-Schlumberger electrode array and electrode spacings of 0.75 and 1 m. ERT depth sections were calculated using the RES2DINV software. Based on the results of ERT studies, vibracoring sites were determined to guarantee maximum information on subsurface stratigraphies and architectural structures. For vibracoring, we used a Nordmeyer automotive drill rig (type RS 0/2.3) and both open and closed coring systems with core diameters of 80 mm and 60 mm. Closed sediment cores were retrieved in plastic inliners with a diameter of 50 mm. Maximum coring depth was 8 m below ground surface (m b.s.) at vibracoring sites OST 6 and 7 (open cores) and 6 m at site OST 7A (inliner core), respectively. At site OST 7A, the uppermost layer down to 1.50 m b.s. consisted of colluvial and alluvial deposits and archaeological debris, as shown in the open core, and was not recovered with plastic inliners in core OST 7A. Coordinates of geophysical transects as well as vibracoring sites were measured using a differential GPS (type Topcon HiPer Pro FC-250) with a horizontal and vertical precision of approximately 2 cm. Inliner cores were opened in the laboratory, photo-documented, and analysed using a multi-proxy approach. Grain size measurements were conducted based on the Köhn sieving and pipette method (Köhn 1929; Barsch et al. 2000). In this paper, we present grain size data of 39 samples retrieved from core OST 7A between 1.77 m and 4.00 m b.s. showing a mean reproduction error of < 2% with regard to original sample weights. For sediment core OST 7A, magnetic susceptibility was measured using a Bartington Instruments MS3 device with a MS2K surface sensor. Concentrations of more than 30 chemical elements were analysed by means of an X-ray fluorescence spectrometer (portable Niton XL3t 900S GOLDD (SOIL mode), Thermo Instruments); here, we present Sr, Ti, and Pb concentrations. Both magnetic susceptibility and XRF measurements were carried out with a resolution of 1–2 cm. Artefacts encountered in sediment core OST 7A were cleaned and photo-ducumented; diagnostic findings were used for archaeological age estimations.

Microfossil analyses with focus on foraminifera were accomplished for 22 samples recovered from sediment core OST 7A in order to determine the sedimentary environment, palaeoecological conditions, and interferences of the palaeoenvironment, for example, by high-energy impact (e.g. Donato et al. 2008; Mischke et al. 2012; Pilarczyk et al. 2014). We classified species with regard to their habitat preferences according to Murray (2006) and Sen Gupta (1999). A volume of 15 ml per sample was pre-treated with H_2O_2 and

subsequently sieved into fractions 125–200 μm, 200–400 μm, and > 400 μm. The determination of foraminifera species and taxa was carried out according to Loeblich and Tappan (1988) and Cimerman and Langer (1991). A binocular and a stereoscopic microscope were used for semi-quantitative analyses.

Radiocarbon dating was carried out for six samples collected from vibracore OST 7A. These samples consisted of unidentified plant remains. Two samples rendered age inversions so that we excluded them from further interpretation (OST 7A/26 PR, OST 7A/29 PR, Table 1). Three out of four remaining samples yielded $\delta^{13}C$ values shifted to heavier C-isotopes which is interpreted as possibly caused by marine plant material. For this reason, we decided to conduct calibration using the marine13 calibration curve. Doing so, we calculated three different scenarios. For scenario a, we used a mean reservoir age of ~ 400 years ($\Delta R = 0$), scenario b is based on data point #221 from the Calib Marine Reservoir Correction Database using a $\Delta R = 31 \pm 60$, and scenario c on the average of data points #220 and #221 from the same database using a $\Delta R = 6 \pm 35$. Both data points refer to the central Tyrrhenian Sea (Stuiver et al. 2019). In all the figures of this paper, we present scenario b ages. Radiocarbon analyses were carried out by the Klaus-Tschira-Laboratory at the Curt-Engelhorn-Zentrum Archäometrie gGmbH at Mannheim, Germany. Further three radiocarbon ages obtained for samples from vibracore OST 6 were added to Table 1 and Fig. 6 according to Hadler et al. (2015: Table 2).

Results: eoarchaeological studies at the navalia-temple complex in Ostia

Geoarchaeological investigations were carried out in the immediate western front of the building remains that were described by Heinzelmann and Martin et al. (2002) as navalia-temple complex of ancient Ostia. Prior to sediment sampling, geophysical site prospection using electrical resistivity tomography (ERT) was accomplished in order to determine best possible vibracoring sites and to better understand subsurface structures (Figs. 4, 5). Sediments retrieved from the site underwent detailed sedimentological, geochemical, microfossil, and geochronological analyses to allow for multi-proxy-based palaeoenvironmental reconstructions (Figs. 6, 7, 8, 9 and 10).

Geophysical site prospection

In this paper, we present results of ERT measurements conducted along three transects. ERT transect OST ERT 9 with an electrode spacing of 1 m was realized in November 2012 parallel to and in an approximate distance of ca. 3 m to the western front of the building remains. Measurements along ERT transects OST ERT 40 and 44 were carried out in September 2013 using a narrower electrode spacing of 0.75 m enabling a higher spatial resolution. Transect OST ERT 9 and 40 were measured in identical direction and position but with different spatial resolution. Both transects entirely cover the area where archaeological sondage 21 was excavated in 2000/2001 (Heinzelmann 2020). Transect OST ERT 44 lies ca. 1.5 m closer to the building front compared to transects OST ERT 9 and 40 (Fig. 4).

Transect OST ERT 9 reveals a threefold pattern. The lowermost part – from NNW to SSE – is characterised by minimum resistivity values ≤ 20 Ωm (blue colours in Fig. 5a). In contrast, the uppermost section generally shows medium values between 17 and 32 Ωm; only in the outermost south-southeastern part of the transect higher values between 33 and 38 Ωm were found (green and yellow colours). The most interesting zone is the intermediate section showing a more or less regular alternation of very high to maximum values (35 to ≥ 53 Ωm, yellow, brown, red, and pink colours) and medium values (26 to 35 Ωm, green, and yellow colours). In this zone, highest values were found towards the SSE.

Depth sections of transects OST ERT 40 and 44 are almost identical. In the SSE, maximum values ≥ 48 Ωm were found extending from close to ground surface to ca. 2 m below sea level (m b.s.l.). Subzones with slightly higher and lower resistivity values alternate within a few meters distance. In contrast, the NNE-sided part of the depth sections are characterised by a thin zone of high resistivity values on top (≥ 34 Ωm) whereas in the intermediate to lower zone, we found a rectangular-type subzone with lower (≤ 23 Ωm, blue colour) resistivity values flanked by subzones with higher values (≥ 33 Ωm, green colours in Fig. 5b, c). As these subzones were considered to reflect relevant resistivity variations in relation with the structure of the building, vibracoring sites were chosen in a way that core OST 6 hits a lower resistivity and core OST 7/7A a higher resistivity rectangular zone. Coring sites were placed right between parallel ERT transects 40 and 44 at distance meters 9.5 m (OST 6) and 13 m (OST 7/7a) with regard to transect OST ERT 44, respectively (Fig. 4).

The sedimentary record of the navalia-temple complex

Stratigraphic record based on vibracoring

Vibracore OST 6 (ground surface at 2.05 m above sea level (m a.s.l.), N 4626011.421, E 273895.984 UTM) was drilled to a depth of 8 m below ground surface. The stratigraphy can be summarized as follows. The lower part of the core is dominated by grey homogeneous clayey silt (up to 4.34 m b.s.) with some medium and coarse sand intercalations towards the top (Fig. 6). The very base of the core (8.00–7.70 m b.s.) is made out of gravel in a sandy matrix showing a very sharp boundary towards the overlying clayey silt unit. The mid-core section is characterised by a thick layer out of (from base to

Table 1 Results of radiocarbon dating (^{14}C AMS) on samples retrieved from sediment cores OST 7A and OST 6 drilled in the outer part of the navalia-temple-complex at ancient Ostia

Sample name	MAMS Lab. No.	Depth (m b.s.)	Depth (m b.s.l.)	Sample description	δ^{13} C (ppm)	^{13}C Age (BP)	1σ max; min (cal BC/AD)	2σ max; min (cal BC/AD)
OST 7A/20 OS	38217	3.17	1.11	Unidentified organic matter	− 12.8	2217 ± 20[a]	89–162 AD	65–218 AD
						2217 ± 20[b]	92–247 AD	18–341 AD
						2217 ± 20[c]	82–194 AD	35–251 AD
OST 7A/26 PR	38218	3.49	1.43	Unidentified plant remain	− 25.3	2617 ± 23	807–795 BC	820–785 BC
OST 7A/29 PR	38219	3.63	1.57	Unidentified plant remain	− 23.3	2409 ± 23	508; 409 BC	728; 404 BC
OST 7A/33 PR	38220	3.76	1.70	Unidentified plant remain	− 18.4	2177 ± 21[a]	139–220 AD	101–252 AD
						2177 ± 21[b]	132–297 AD	70–386 AD
						2177 ± 21[c]	133–244 AD	77–305 AD
OST 7A/36 PR	38221	3.85	1.79	Unidentified plant remain	− 11.9	2204 ± 19[a]	100–179 AD	80–228 AD
						2204 ± 19[b]	102–259 AD	33–352 AD
						2204 ± 19[c]	98–210 AD	51–263 AD
OST 7A/39 PR	38222	3.97	1.91	Unidentified plant remain	− 24.7	2513 ± 25	773; 560 BC	790; 542 BC
OST 6/13 HR*	19760	3.88	1.84	Piece of wood	− 33.8	2101 ± 20	168–94 BC	181–53 BC
OST 6/19+ HR*	19761	4.56	2.52	Piece of wood	− 24.9	2168 ± 20	349; 180 BC	356; 166 BC
OST 6/27+ PR*	19762	7.42	5.38	Unidentified plant remain	− 24.6	2191 ± 20	353; 202 BC	359; 194 BC

Note: b.s.—below ground surface; b.s.l.—below present mean sea level; 1 σ (2σ) max; min cal BP/BC (AD)—calibrated ages, 1 σ (2σ)-range; ";"—total interval between minimum and maximum calibrated ages; age model shows multiple intersections with the calibration curve; calibration based on Calib Rev 7.1.0 software (Reimer et al. 2013); Marine Reservoir Effect (MRE) considered for calibration using the marine13 calibration curve: [a] mean reservoir age of ~ 400 years (ΔR = 0); [b] data point # 221 from Calib Marine Reservoir Correction Database (ΔR = 31 ± 60); [c] average from data points # 220 and 221 from Marine Reservoir Correction Database (ΔR = 6 ± 35); * original data published by Hadler et al. (2015); Lab. No.—laboratory number: Klaus-Tschira-Labor, Curt-Engelhorn-Zentrum Archäometrie gGmbH, Mannheim, Germany (MAMS)

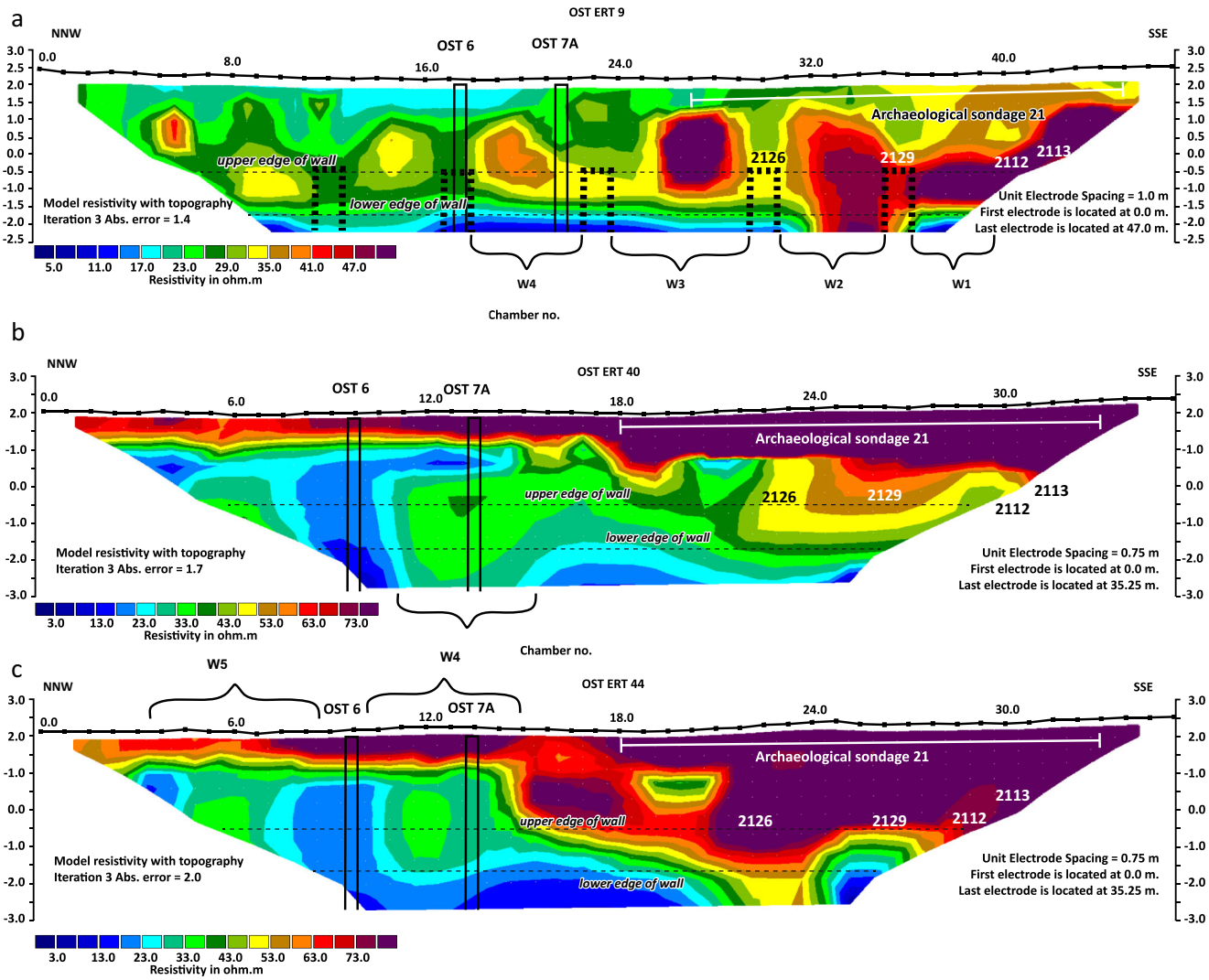

Fig. 5 Depth sections of electrical resistivity tomography (ERT) measurements along transects in the immediate front of the navalia-temple complex at ancient Ostia. For location of transects see Figs. 1, 3 and 4. See text for further explanations

top) coarse, medium, and fine sand (4.34–3.80 m b.s.) and another layer of medium and coarse sand (3.80–3.70 m b.s.). These sands immediately underlie a very striking and thick unit from 3.70–2.62 m b.s. made out of alternating blackish brick and greyish mortar sublayers which obviously document a wall that was completely penetrated (Fig. 6). On top, we found another reddish brick layer (2.62–2.57 m b.s.) that is covered by brownish to beige-coloured silty fine sand (2.57–1.57 m b.s.) and greyish light-brown clayey silt until the top (1.57–0 m b.s.). In core OST 6, we found several ceramic fragments, namely, a prehistoric coarse-grogged fragment in the basal gravel (7.73 m b.s.), as well as several fragments dating to mid-Republican to Imperial times (ca. third century BC to third century AD), the lowermost found at 4.64 m b.s.

Vibracore OST 7 (ground surface at 2.06 m a.s.l., N 4626007.944, E 273896.606 UTM) shows a stratigraphy quite similar to the one found at neighbouring site OST 6 (Fig. 6). The lowermost part is made out of fine gravel (7.95–7.76 m b.s.) followed by a thick unit of homogeneous clayey silt (7.76–4.45 m b.s.) with intersecting sand layers in its upper part. From 4.45–3.98 m b.s., we found grey, fining-upward medium to fine sand including muddy rip-up clasts and covered by grey silty clay (3.98–3.84 m b.s.). The middle section of the core (3.84–2.90 m b.s.) is dominated by blackish grey to grey medium and fine sand showing layering structures. On top, we encountered sand and gravel including ceramic fragments and mosaic pieces (2.90–2.65 m b.s.) covered by grey to beige-coloured fine to medium sand (2.65–2.43 m b.s.). Similar to OST 6, the uppermost units are made out of brown to beige-coloured silty clay (2.43–1.60 m b.s.) and light brown clayey silt (1.60–0 m b.s.). Several ceramic fragments dating to mid-Republican to Imperial times (third century BC to third century AD) were found in the core, the lowermost ones at 4.44 m and 4.23 m b.s.

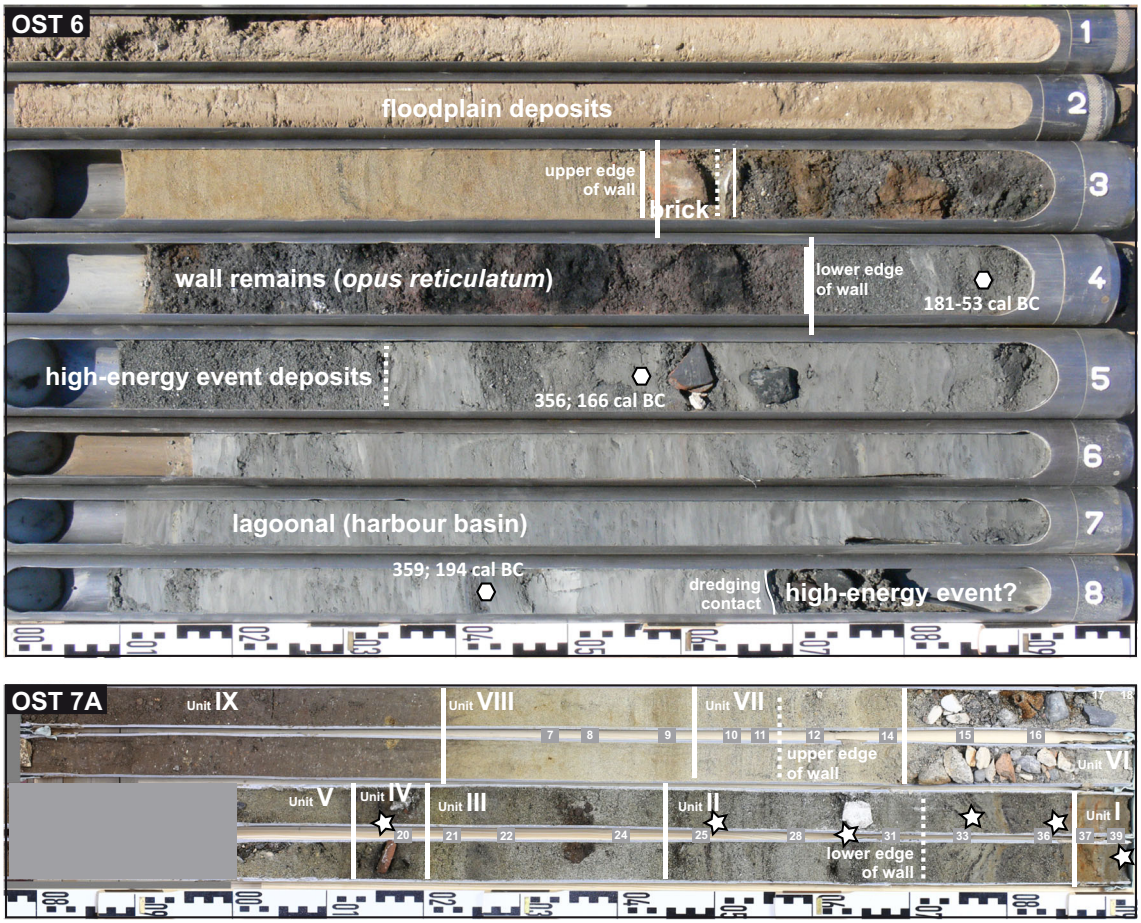

Fig. 6 Photographies of vibracores OST 6 and OST 7A. *core* OST 6 penetrated an *opus reticulatum* wall that originally separated vaulted chambers of the navalia-temple complex. Radiocarbon ages are given according to Hadler et al. (2015). Core 7A shows the sedimentary infill of chamber W4. Hexagons mark position of radiocarbon samples retrieved from core OST 6 with calibrated ages (2σ) already published by Hadler et al. (Hadler et al. 2015; see Table 1). Asterisks mark position of samples retrieved from core OST 7A for radiocarbon dating (see Table 1). Upper and lower edge of the *opus reticulatum* wall found in core OST 6 are marked by dashed lines in core OST 7A. For location of vibracoring sites see Figs. 1, 3, 4 and 5. Photos: A. Vött, T. Willershäuser

Vibracore OST 7A was drilled as closed inliner core version of OST 7 focusing on the section crucial for the relation between navalia-temple-complex and palaeoenvironmental setting. The core starts at 1.50 m b.s. and ends at 4.00 m b.s., this section being used for detailed multi-methodological analyses (Fig. 6). The stratigraphy is classified into nine units (I to IX, Fig. 6). Unit I (4.00–3.86 m b.s.) is made out of grey to brownish grey fine sandy clayey silt. It is covered by unit II (3.86–3.44 m b.s.) which is characterised by alternating thin layers out of blackish to beige-coloured grey silt, fine, medium ,and coarse sand, and, on top, fine gravel. Subsequent unit III (3.44–3.20 m b.s.) is a massive brownish grey medium sand with coarse, fine sand, and silt. Unit IV is striking, because it is a thin silt-dominated layer of brown to blackish-brown colour (3.20–3.12 m b.s.) including a fragment of an ancient amphora, indeterminable in age (Figs. 6 and 9f). It is covered by massive beige-coloured grey medium and fine sand (3.12–3.00 m b.s.). The subsequent unit VI (3.00–2.70 m b.s.) is dominated by gravel and coarse sand, whitish to light grey in appearance, including a Roman nailhead at 2.81 m b.s. (Fig. 9b). Unit VII (2.70–2.47 m b.s.) is dominated by whitish beige-coloured fine sand with subordinate medium sand, thinly laminated, and also including fine gravel and dark heavy mineral grains. On top, we found comparatively well sorted fine sand (unit VIII, 2.47–2.22 m b.s.), slightly laminated in the lower and massive in the upper part. This unit is covered by silty fine sand (base) and fine sandy clayey silt (top) of unit IX (2.22–1.77 m b.s.), both coloured brown to dark brown. The uppermost section from 1.77–1.50 m b.s. is missing due to sediment compaction of the stiff and solid silt- and clay-dominated brown top layer (unit IX).

Comparing the stratigraphy of vibracore OST 7A with the wall penetrated by core OST 6, the lower edge of the wall ends in the lower third of unit II at 3.72 m b.s., whereas the upper

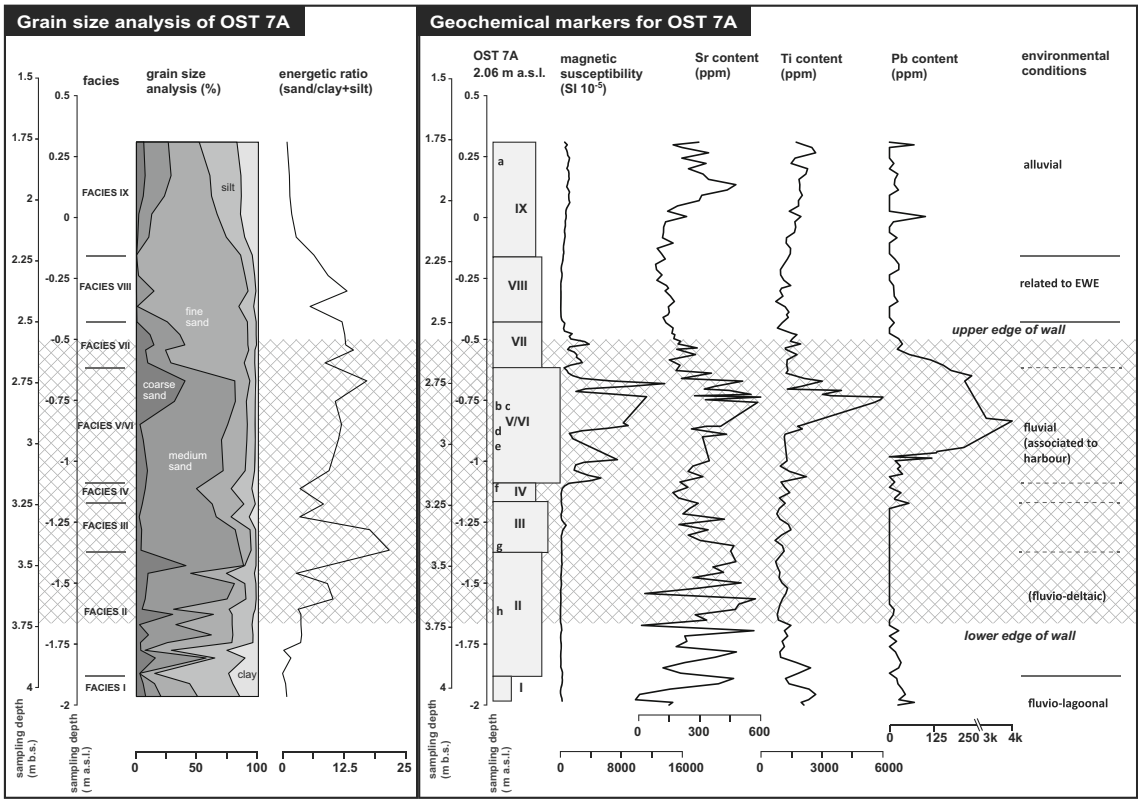

Fig. 7 Selected sedimentological and palaeoenvironmental proxies obtained for sediment core OST 7A. Lowercase letters in the stratigraphic log mark artefacts found in core OST 7A and depicted in Fig. 9. For information on methodological details see text

edge of the wall at 2.56 m b.s. lies in the midst of unit VII. In total, the wall thus faces stratigraphic units II to VII of core OST 7A (Fig. 6).

Multi-proxy sediment core analysis and grain size data

Selected palaeoenvironmental parameters collected for vibracore OST 7A are summarized in Fig. 7. Grain size distribution shows that unit I is dominated by low-energy fine-grained silts and clay, whereas unit II is characterised by alternating layers of silts and sands. In contrast, units III to VI show medium and coarse sand as predominant grain size classes. Units VII and VIII are strongly dominated by fine sands. Finally, unit IX is an uniformly mixed deposit comprising all grain size classes. The energetic level represented by the sediments encountered is very high for units II to VIII, very low for unit I and moderate for unit IX. Detailed results of grain size analyses are depicted in Fig. 8 showing the grain size character of the sediment units and their different degrees of sorting. Also, the clear shift from predominant medium sand in units II to VI (Fig. 8b, e) to fine sand in units VII and VIII (Fig. 8f, g) can be clearly seen. Sorting appears best for sediments of units III and V, followed by units VII and VIII.

Magnetic susceptibility values remain on a very low level for sediments of units I to IV (Fig. 7). Maximum values were found for units V and VI with only slightly lower values encountered for unit VII. Units VIII and IX show minimum values again. Sr concentrations are highest in units II, III, V, and VI as well as in the uppermost part of the core, whereas units I, IV, and VIII show clear minima. Moreover, Ti values appear with a clear maximum for unit VI whereas values for other units are on a uniformly lower level. Apart from low concentrations in unit I and the lower section of unit II, Pb values strongly increase with the onset of unit IV and find their maximum in units V, VI and the lower part of unit VII. The top of the core again shows low Pb values apart from individual higher peaks towards the top.

Artefacts found in vibracore OST 7A are marked with lowercase letters in Fig. 7 and are depicted in Fig. 9. Unfortunately, none of the findings can be used for high-resolution dating, but one can only assert that all of them attest to Roman times. However, artefacts spread over almost the entire sediment core. Only unit I was found void of any anthropogenic findings.

Microfaunal studies

Results of micropalaeontological studies are summarized in Fig. 10. Species and taxa encountered in sediments of vibracore OST 7A were grouped into three main environments (fully marine, marine to shallow marine, lagoonal) for which the presented individuals are most typical. Also, we consider

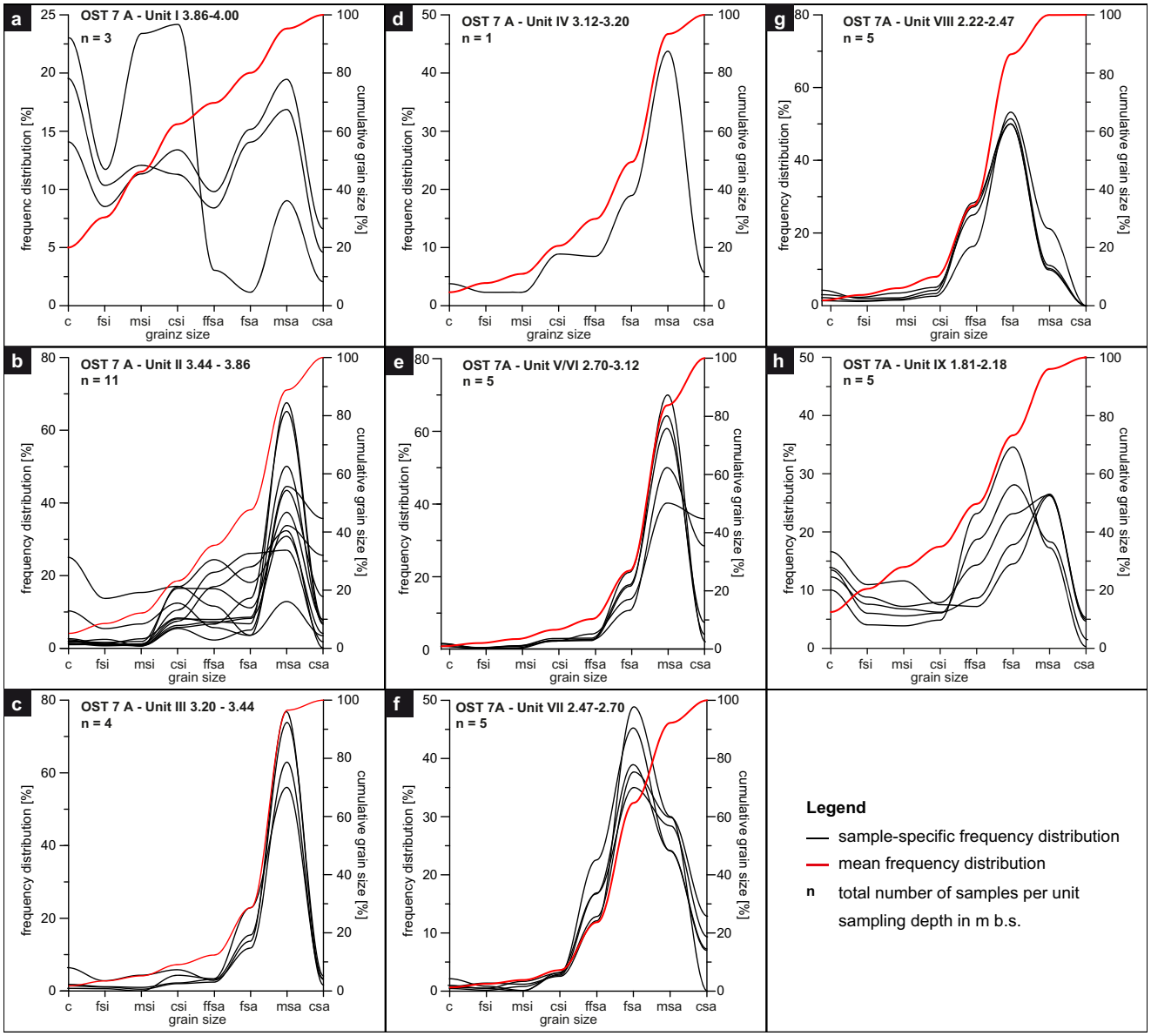

Fig. 8 Frequency distributions of grain size data as well as cumulative grain size data obtained for sediment samples from core OST 7A. Samples are grouped according to stratigraphic units I to IX. See text for further information

Globigerinoidae as well as *Orbulina universa* as most probably reworked.

In general, the foraminiferal and thus environmental signature found for units I to VI is similar – there are no big differences in the number of species and taxa. However, *Cassidulina* sp., *Cibicidoides* sp., *Bulimina* sp., *Elphidium* sp., *Ammonia tepida* and *Haynesina* sp. show higher abundances in sediments of unit I and the lower part of unit II compared to the remaining section of unit II and units III, IV, V, and VI. This seems to document a slightly stronger influence of salt water for the lowermost part of vibracore OST 7A. The only taxa that was not found in unit I and the lower part of unit II is *Adelosina* sp. what might be due to differing demands on saltwater conditions.

Considering the entire core section that was subject to microfaunal studies, both abundance and diversity of species and taxa were found lowest for sediments of units III, V, and VI. It is striking that both abundance and diversity show clearly defined maxima for sediments of units VII and VIII. The number of species found here is up to double as high as in the sediments below. The strong marine signature related to units VII and VIII is more than obvious: *Cassidulina* sp., *Cibicidoides* sp., *Gyridinoides* sp., *Hyalinea* asp., *Melonis* sp., *Pullenia* sp., *Uvigerina* sp., *Bulimina* sp., *Cibicides* sp., *Elphidium* sp., *Eponides* sp. and *Haynesina* sp. show very

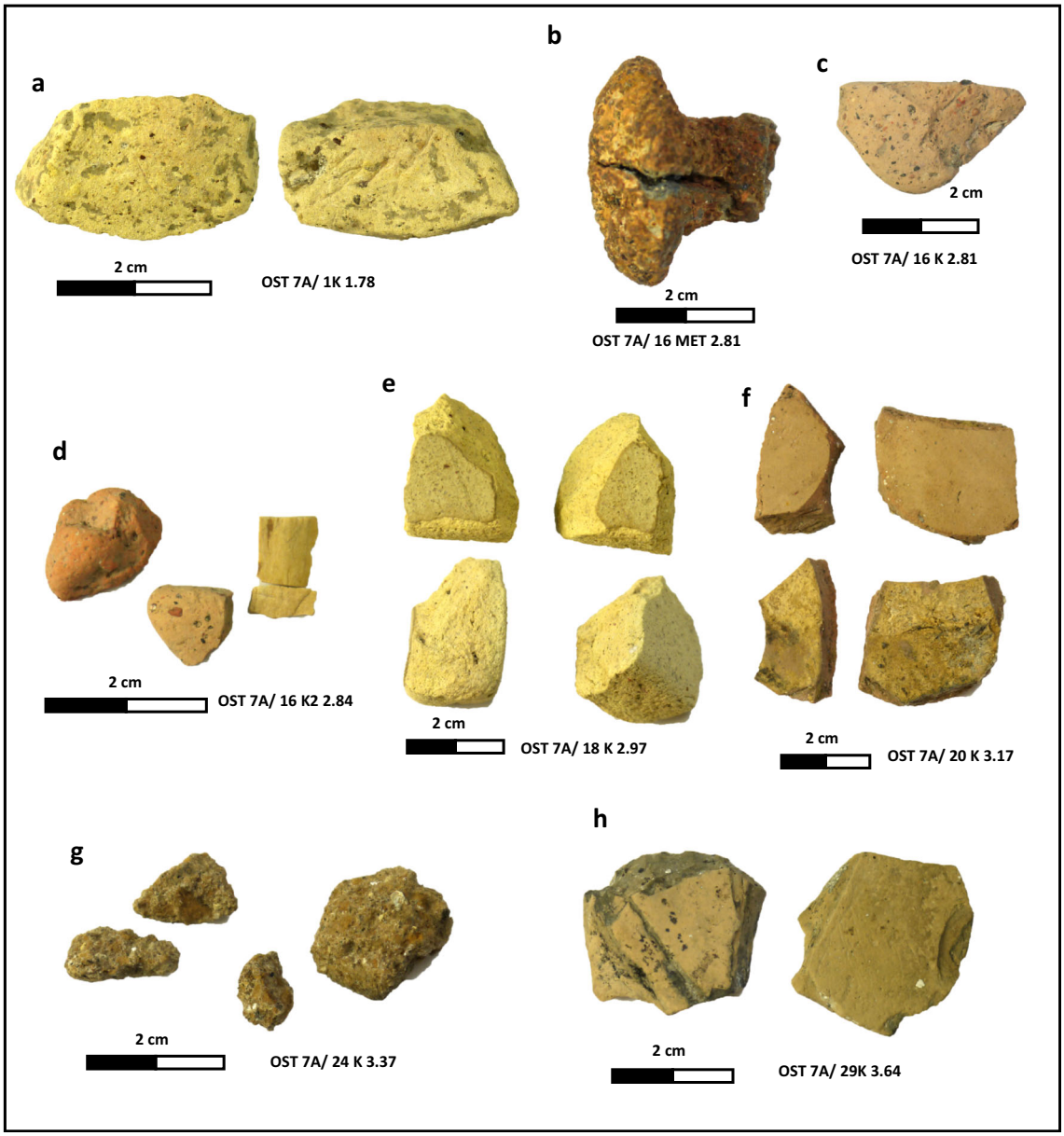

Fig. 9 Photos of artefacts found in vibracore OST 7A. See text for further details

clear maxima in abundance in units VII and VIII compared to the sediments below. Moreover, species and taxa of *Ammonia beccarii*, *Neoconorbina* sp., *Nodosaria* sp., *Nonion* sp., *Rosalina* sp., *Valvuleria* sp. were exclusively found in units VII and VIII – apart from individual, sporadic findings of some of these taxa in the lower core section.

The distribution pattern of microfaunal remains retrieved from core OST 7A thus reflects the evolution of a saltwater-influenced near-coast environment close to the River Tiber (unit I, lower part of unit II) towards an environment with decreased saltwater influence but steadily high flow energy (upper part of unit II, units III to VI). The onset of unit VII finally marks the abrupt and strong increase of marine foraminifers due to a sudden intrusion of marine waters.

Geochronological data

Results of radiocarbon dating are summarized in Table 1 and depicted in Fig. 10 in the stratigraphic context. The calibrated radiocarbon age yielded for unit I is 790–542 cal BC. The subsequent three radiocarbon ages (scenario b) for units II and IV are quasi-identical within the range of error, namely 33–352, 70–386, and 18–341 cal AD. This remains also true if one considers scenario a or scenario c ages (Table 1). The corresponding sediments were thus deposited within a short

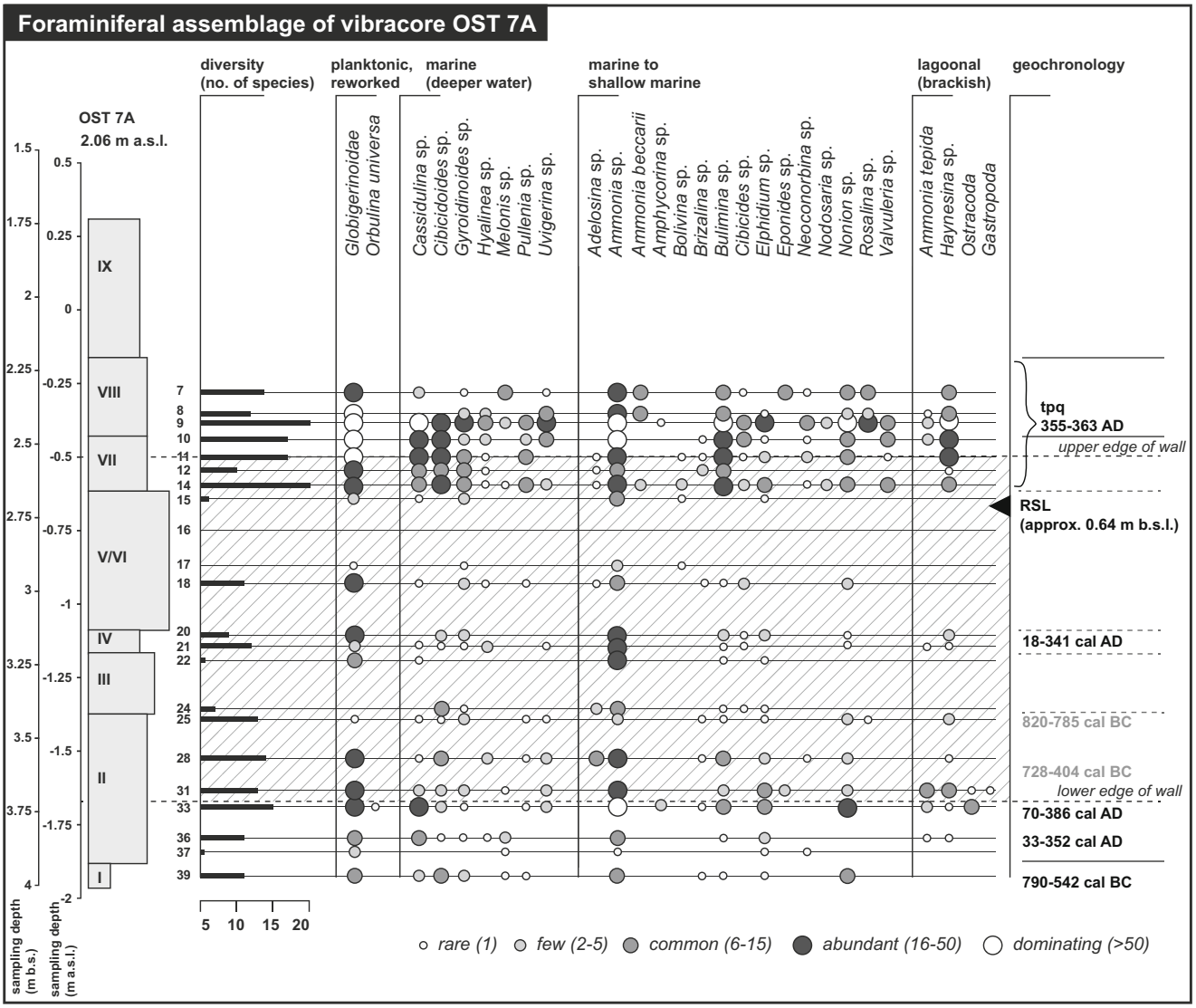

Fig. 10 Results of microfossil analyses conducted for sediment samples from vibracore OST 7A. Small figures to the right of the stratigraphic log indicate sample numbers. The hatched area marks sediments facing the *opus reticulatum* wall penetrated in neighbouring core OST 6. Note strongly increased abundance and diversity found for samples of stratigraphic units VII and VIII. The increase is interpreted as the effect of a tsunami landfall. Further information, see text

time span at some point of time between, at most, the first and the fourth century AD. Two further samples retrieved from unit II yielded age inversions and are not included in age interpretation.

Discussion

Facies determination for sediment cores from the navalia-temple complex

Based on sedimentary, geochemical, mineralogical, and palaeoenvironmental data obtained from multi-proxy analysis, we interpret the stratigraphic units of vibracore OST 7A in terms of sedimentary facies as follows.

The lowermost unit I reflects low-energy sedimentary conditions with the predominant accumulation of silt and clay. High Sr values and microfossil data attest to a marine influence. However, conditions are not fully typical of purely lagoonal conditions (Fig. 10) so that a considerable inflow of water from the River Tiber must be assumed. We, therefore, characterise this unit as fluvio-lagoonal facies.

The lower part of unit II marks the change from the low-energy to a higher-energy environment (Fig. 8b) in which considerable and increasing amounts of sand are transported. The marine influence still remains visible but continuously decreases towards the top of unit II (Fig. 10). We interpret this as the consequence of increasing river water influence to the system. Conditions remain similar throughout units III, IV, V, and VI but with

decently decreased water inflow from the marine side. Saltwater influence was found lowest for units V and VI so that – here – purely fluvial conditions have to be assumed. Fluvial impact is also attested by highest amounts of coarse-grained sediments, especially medium, and coarse sands, found associated with the entire core section from unit II to unit VI. Maximum values for magnetic susceptibility and Ti concentrations appear to be due to major influence from the River Tiber that brings along volcanogenic components as well as weathering products from eroded rocks and soils from upstream (mountainous) regions. In contrast, maximum Pb values may be only partly assigned to natural influences; they seem to be mainly caused by human impact at Ostia itself. Lead (Pb) was typically used in the form of tubes and clamps. Furthermore, the interior of ships was often riveted with sheets of lead in order to improve their stability. In summary, the sedimentary facies encountered in units II to VI is, therefore, determined as fluvio-deltaic (lower part of section II) to predominantly fluvial (upper part of unit II, units III to VI) with considerable human impact. The latter seems clearly associated with the use of the site as river harbour.

The transition from unit VI to unit VII is characterized by the abrupt shift from medium sand to fine sand as dominant grain size (Fig. 8e, f). Moreover, the mineralogical and geochemical signature as depicted by proxies in Fig. 7 shows a clear dilution effect – magnetic susceptibility as well as concentrations of Ti and Pb are strongly decreased (unit VII) or almost nil (unit VIII). Microfossil data prove an abrupt and very strong increase of both abundance and diversity of marine species and taxa (Fig. 10) compared to underlying fluvial sands. Moreover, the foraminifer assemblage shows a mixture of species and taxa from different saltwater-dominated environments. Thus, we interpret units VII and VIII to be caused by the impact of an extreme wave event (EWE) from the seaside, namely, by storm or tsunami. Terrigenuous or fluvial impacts still seems to be higher in unit VII because magnetic susceptibility values and Pb concentration are higher than measured for unit VIII. This can be interpreted as the consequence of a first seawater pulse arriving at the harbour and mixing the River Tiber waters and sediments with those of littoral and marine origin. However, magnetic susceptibility values may also be influenced by the mobilization of heavy mineral depots in the immediate coastal zone. In contrast, unit VIII sands are characterised by a purely marine signal and might be explained by a second sea water impulse hitting the harbour. Finally, it is striking that unit VIII sands appear completely identical in texture and colour with littoral fine sands from the present-day coast some 3 km to the southwest of ancient Ostia.

Overall, we finally interpret units VII and VIII as related to a possibly two-pulsed extreme wave impact to Ostia's harbour from the seaside.

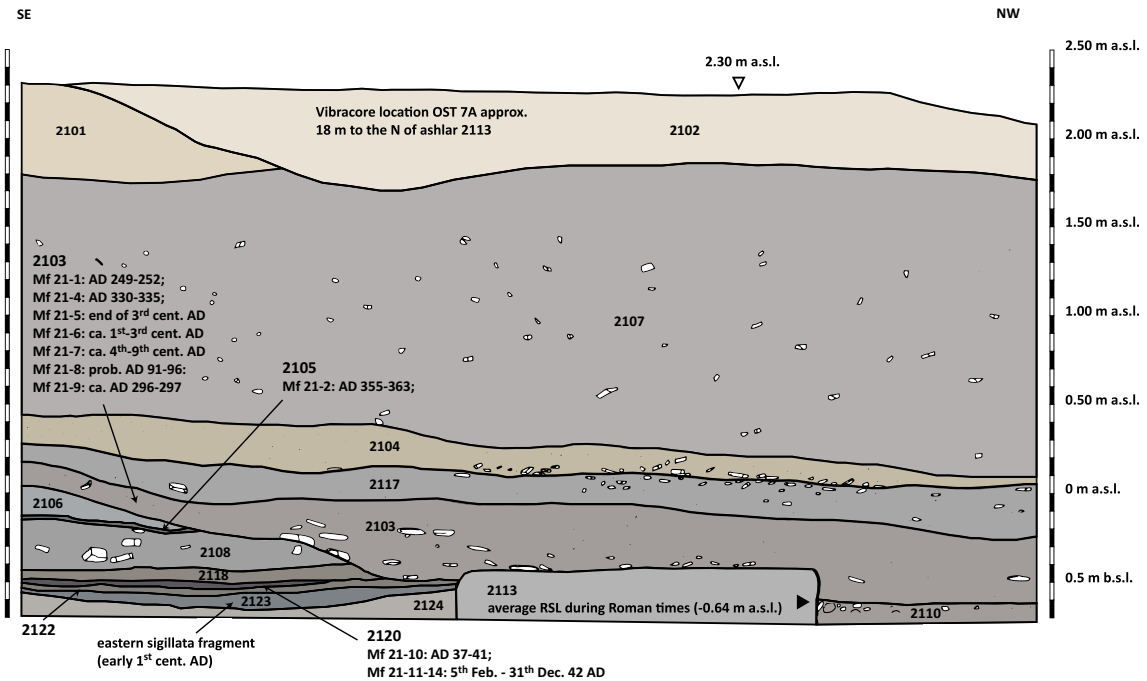

Fig. 11 Cross section of the southwestern face of archaeological sondage 21 adapted from Heinzelmann (2020). Numbers (2102 etc.) document strata as described during archaeological investigations. Mf – coin finding and coinage date. RSL – relative sea level, reconstructed based on geomorphological sea level indicators. See text for further information. All data (except RSL) from Heinzelmann (2020)

According to its brown colour, mixed grain size classes as well as individual Pb peaks towards the modern surface, we interpret unit IX as alluvial facies deposited during flood events by the River Tiber.

Geochronostratigraphic units recovered by archaeological excavations

During excavation of archaeological sondage 21 in 2000/2001, the archaeological and lithological stratigraphies were studied in detail. Fig. 11 gives an overview of the individual stratigraphic units observed at the SE-NW striking sondage wall (view to the W) as reported by Heinzelmann (2020). Here, we give a short description of the stratigraphic units from bottom to top including the original numbers for strata and ashlars presented by Heinzelmann (2020). The focus is laid on those units that render chronostratigraphic information and that are required for stratigraphic comparison with vibracore OST 7A.

Units 2127 and 2134 (not depicted in Fig. 11) document the oldest units observed. They were found to the immediate east of ashlar 2129 and to the north and south of wall fragment 2128, respectively (Fig. 4). These units are made out of very compact *opus caementicium* and represent the original floor of the vaulted chambers. Heinzelmann (2020) states that this floor increased in height from west to east and estimates the inclination to be ca. 5°.

Unit 2123 (Fig. 11) is made out of sand and includes abundant marble fragments that were possibly produced during the construction of the navalia-temple complex. The unit also included fragments of eastern sigillata from the early first century AD. Heinzelmann (2020) interprets unit 2123 as contemporaneous to the first period of use of the navalia-temple complex.

Further towards the top, unit 2120 is a compact reddish beige-coloured former surface found to the south of wall segment 2116 (Fig. 4). It also included many tuff fragments. According to Heinzelmann (2020), this layer represents a second phase of use of the building complex. The following coins were found in this unit with the period of coinage during the reign of the corresponding emperor given in brackets: Mf 21–10, Caligula (AD 37–41); Mf 21–11 to 21–14, Claudius (AD 5th February 42 – 31st December 42). The latter coins were considered as *termini ad quos* so that the unit can be dated to the reign of Claudius, namely, to the midst of first century AD.

The next characteristic layer is unit 2105 that is described as a sandy sediment. It was only found in some parts of sondage 21, namely, to the immediate north of wall 2116. This layer also included ceramic and brick fragments as well as a coin, Mf 21–2, imprinted under an undetermined ruler, showing AD 355–363 as coinage date. Together with a rubble layer on top (unit 2106) that included numerous fragments of hydraulic mortar and brick fragments from *opus spicatum*, units 2105 and 2106 are both cut by unit 2103 (Fig. 11) resulting in a *terminus ad* or *post quem* for the depositional age of unit 2103 of AD 355–363. Heinzelmann (2020) interprets unit 2105 as representing the last period of use of this part of the navalia-temple complex.

Unit 2103 itself is made out of blackish sand found all along sondage 21 with high contents of magnetite that, after Heinzelmann (2020), were originally transported to Ostia from volcanic regions to the east of Rome by the River Tiber. Layer 2103 also included higher quantities of ceramics and building material that were obviously rounded by transport processes. The following coins were included in this unit: Mf 21–1 Trajanus Decius (AD 249–252), Mf 21–4 Constantin II as Caesar (AD 330–335), Mf 21–5; Gallic fake of Nummus Claudius (end of third century AD), Mf 21–6; not identifiable (probably first to third century AD), Mf 21–7: not identifiable (probably fourth to fifth century AD), Mf 21–8; Quadrans (probably AD 81–96), Mf 21–9: Diokletian (ca. AD 296–297). Considering secure dating information, the coins yield a *terminus ad* or *post quem* for the deposition of the sand of AD 330–335.

The subsequent unit 2117 is made out of light grey sand, loose in consistency, and was found everywhere in sondage 21 right between units 2103 and 2104. Unit 2104 consists of dark beige-coloured sand and was also encountered all along sondage 21. According to Heinzelmann (2020), both colour and consistency suggest that the material originates from sandy beaches around the Tiber River mouth. The sediment was mostly sterile. Only one fragment of Italic sigillata (ca. 30 BC) was found and is considered redeposited.

On top of layer 2104, unit 2107 is described as humic brown loamy material that could be traced all along the sondage. Heinzelmann (2020) suggests that it results from colluvial and alluvial depositional processes. A fragment of African lustre ceramic (ca. AD 70) is obviously redeposited and, therefore, only yields a rough *terminus post quem* for this unit.

Unit 2110 is described from the immediate north of ashlar 2113 as compact, mixed black, and beige-coloured sand found all along sondage 21 that included many rounded fragments of bricks, *opus reticulata*, marble, and ceramics. During excavation in 2000/2001, it partly lay below the groundwater level. Heinzelmann (2020) assumes that the layer was probably deposited in the course of late- or post-ancient siltation of the harbour basin.

At its western side, ashlar 2113 shows sea level-related outwash marks (Heinzelmann 2020). Similar features caused by sea level influence were observed at ashlars 2126 and 2129, namely, at the sides facing the harbour basin (Fig. 4). We re-calculated the data given by Heinzelmann (2020) using high-precision DGPS measurements carried out within the study presented in this paper, so that we were able to reconstruct the relative sea level stand at the time of use of the building to ca. 0.64 m b.s.l. (Fig. 11).

Synthesis of archaeological and geoarchaeological data

Results from ERT measurements (Figs. 3, 5) suggest that the wall penetrated by core OST 6 corresponds to one of the walls separating vaulted chambers of the navalia-temple complex as described above and by Heinzelmann (2020). Also, the structure of the wall penetrated by core OST 6 (Fig. 6) is identical with the structure of an *opus reticulatum* as described in archaeological literature and as can be originally seen in the accessible northern vaulted chambers (Fig. 3d–f). Even one out of originally six brick layers of the *opus latericium* observed on top of the *opus reticulatum* is preserved in core OST 6 (Figs. 3, 6).

Fig. 5a is, therefore, interpreted in a way that vibracore OST 6 hit the *opus reticulatum* wall between vaulted chambers W4 and W5, whereas vibracore OST 7A yielded the infill of the vaulted chamber W4 itself. Resistivity values found for the penetrated wall segment are considerably smaller than those associated with the sedimentary infill of the chamber. This is because the wall is mostly made out of clay-born bricks whereas the infill sediments are dominantly sandy; both sucked with groundwater, the finer-grained material shows a higher conductivity than the relatively coarse-grained sand that partly fills the chamber. This is corroborated by the results of ERT transects OST ERT 40 and 44 (Fig. 5b, c) and corresponds with the overall experience concerning the interpretation of ERT data (Fischer et al. 2016, Obrocki et al. 2019).

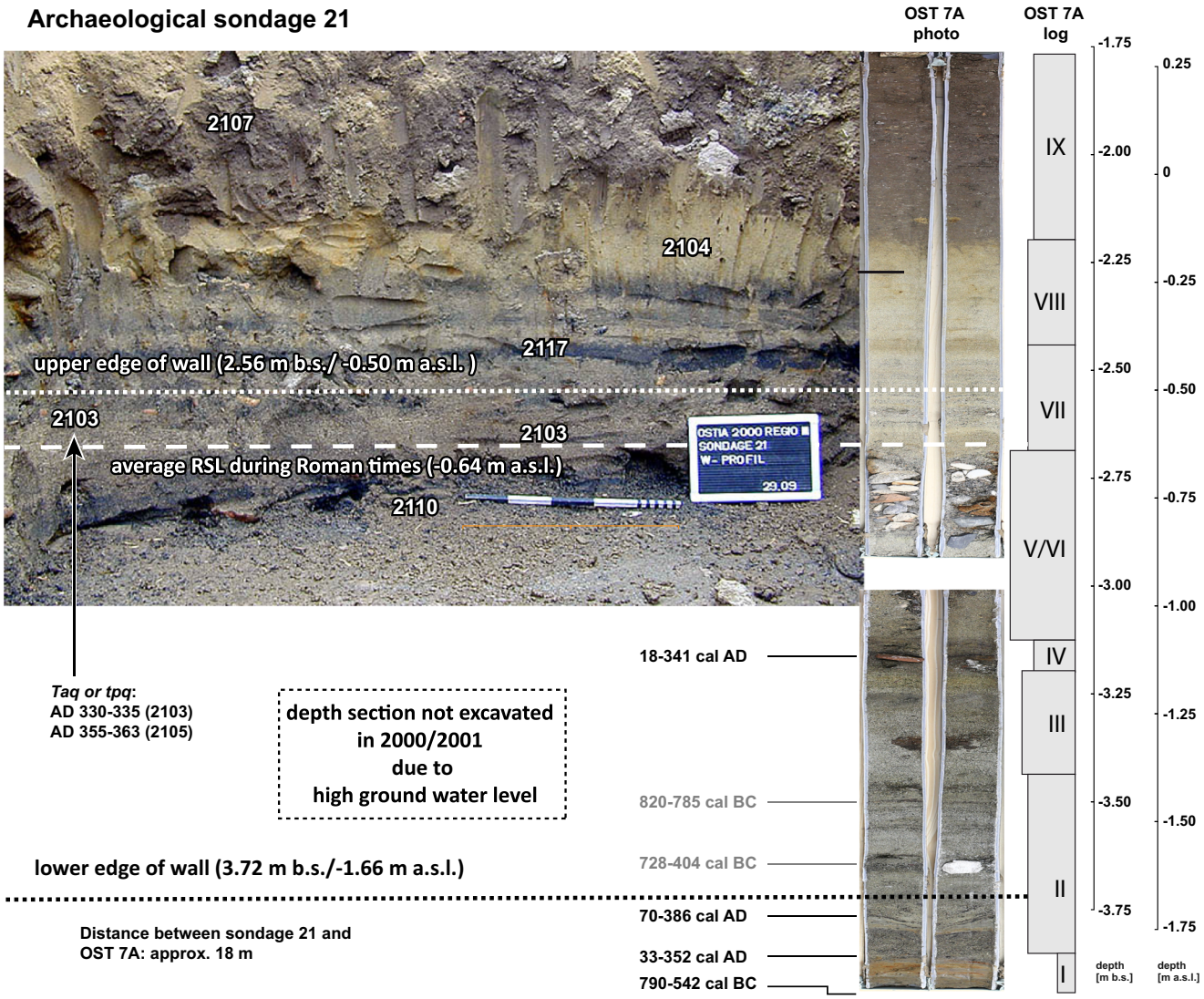

Fig. 12 Synopsis of archaeological and geoarchaeological data obtained from the western front of the navalia-temple complex. Photo of western face of archaeological sondage 21 with original strata numbers after Heinzelmann (Heinzelmann 2020; see also Fig. 11). Note that vibracore OST 7A yields information on sections below groundwater that could not be excavated in 2000/2001. *taq – terminus ante quem*, *tpq – terminus post quem*

Archaeological sondage 21 covers vaulted chambers W1, W2, and W3 as shown in Figs. 2, 4, 5. The depth section of transect OST ERT 45 (Fig. 4 shows direction of transect, the depth section itself is not depicted) did not yield any evidence of walls or chambers further westward so that archaeological and geoarchaeological results are in full accordance: the general idea of the western end of the building is shown in Fig. 2. ERT data presented in this paper further document that large parts of the western front of both the vaulted chambers and the separating walls were subject to erosion after the navalia-temple complex came out of use and, later, were covered by alluvial deposits.

Vibracore OST 7A was drilled ca. 18 m to the north of ashlar 2113 in sondage 21 (Figs. 5, 11, 12). As shown in Fig. 12, the stratigraphy of sondage 21 can be clearly identified in core OST 7A. Archaeological unit 2110 (after Heinzelmann 2020, see also Fig. 11) represents unit VI in core OST 7A. Archaeological units 2103 and 2104 are identical with the stratigraphic units VII and VIII, respectively, whereas unit 2117 is included in stratigraphic unit VIII (Fig. 6). Finally, archaeological unit 2107 corresponds to OST 7A stratigraphic unit IX (Fig. 12).

Vibracore OST 7A delivers information on considerably deeper stratigraphic units compared to archaeological sondage 21 as the latter had to stop when the groundwater level was reached. During the dry summers in 2000 and 2001, when the discharge of the River Tiber was low, this was around 0.75 m b.s.l. This results in the fact that stratigraphic units I to V of vibracore OST 7A lie beyond the bottom of sondage 21. Thus, the entire sedimentary sequence associated with the brick wall penetrated in core OST 6 (Fig. 6) can be assessed in detail.

In fact, vibracore OST 7A goes some 28 cm deeper than the lower edge of the *opus reticulatum* wall between vaulted chambers W4 and W5 (final coring depth of core OST 7A, 1.94 m b.s.l.; lower edge of wall, 1.66 m a.s.l.). This also allows, to some extent, to draw conclusions on the pre-harbour situation near the navalia-temple complex.

Finally, comparing archaeological information from sondage 21 and the stratigraphy of vibracore OST 7A documents that the relative sea level during the first half of the first century AD, when the first phase of use of the navalia-temple complex is documented (see above), lies at approx. 0.64 m b.s.l. and thus right in the transition between stratigraphic units VI and VII as encountered in core OST 7A (Fig. 12).

The history of Ostia's river harbour and the navalia-temple complex and how long they were in use

Using a geoarchaeological approach, we were able to identify further originally vaulted chambers and the *opus reticulatum* walls between them (Fig. 5). Vibracore OST 6 was drilled right through an ERT anomaly found in transects OST ERT 9, 40, and 44 that turned out to be the wall between chambers W4 and W5 (Figs. 2, 3, 5). We also obtained a view underneath the base of the building itself way below the present-day seasonal ground water level. Based on the multi-proxy analysis of sediments from vibracore OST 7A that were retrieved from chamber W4 – directly facing the penetrated wall found in core OST 6 – we are now able to reconstruct the history and evolution of the harbour-sided front of the navalia-temple complex at Ostia as follows.

The fluvio-lagoonal facies I encountered in core OST 7A corresponds to the pre-river harbour lagoon-type environment that was already identified by Goiran et al. (2014) and Vött et al. (2015) and which was used as first harbour generation to the west of Ostia at least until the second century BC (Hadler et al. 2015). For core OST 6, corresponding radiocarbon ages are illustrated in Fig. 6 and Table 1 (Hadler et al. 2015). In core OST 7A, such lagoonal sediments represent the base for overlying fluvial deposits of the navalia-temple complex, the latter being considerably younger and lying on top of a hiatus (Fig. 12). This large time gap between the two lowermost radiocarbon ages obtained for core OST 7A (Fig, 12, Table 1) let us suggest that the base of chamber W4 was originally dug out from older (lagoonal) deposits or dredged during a later phase of use of the building. This is supported by the fact that the base of fluvial facies II reaches some 14 cm deeper (1.80 m b.s.l.) than the lower edge of the *opus reticulatum* wall (1.66 m b.s.l.). Further towards the east, one has to expect the base of the chamber being paved with *opus caementicium* as found in layers 2127 and 2134 by Heinzelmann (2020; sondage 21). In contrast, core OST 6 shows that the wall itself was built right on top of a layer out of coarse to medium sand which is interpreted by Hadler et al. (2015), based on sedimentary, microfaunal, and geochronological evidence, as tsunami-related deposits. This high-energy layer could be traced all over the harbour basin both by vibracoring (Hadler et al. 2015; Vött et al. 2015) and seismic reflection measurements (Wunderlich et al. 2018). It can thus be reliably excluded that the sand layer below the wall in core OST 6 has been artificially dumped as foundation material for the building. The pre-navalia tsunami layer was dated by Hadler et al. (2015) to the time before the first half of the first century AD. The sample that yielded the radiocarbon age shown in Fig. 6 is considered reworked by high-energy processes and represents a *terminus post quem*.

The fluvial facies I in chamber W4 that was found directly associated with the harbour use of the building and facing the OST 6 *opus reticulatum* wall forms a geochronological entity. The three radiocarbon samples retrieved from this unit yield ages extending over one and the same time period between the first and fourth century AD within the range of error (Table 1, Figs. 6, 10, 12). The 2σ-maximum age lies close to the time, when the navalia-temple complex was built, namely the

second quarter of the first century AD (Heinzelmann and Martin 2002). The minimum age frame as given by the radiocarbon ages lies between AD 341 and AD 386 (2σ values). Geochemical and mineralogical parameters as well as microfaunal data and ceramic findings clearly document a fluvial facies under distinct man-made influence within a harbour building (Figs. 6, 7, 9, 10).

We, therefore, are able to state that the harbour and its building must have been in use in the given time frame, namely, between the first and fourth century AD. This is in full accordance with archaeological data from sondage 21 (Fig. 11) that allowed to identify two early phases of use of the building in the early first century AD, possibly associated with the construction itself, and the mid-first century AD. The last phase of use was dated by findings of a coin to at or shortly after AD 355–363 (Heinzelmann 2020).

Comparing the base of the fluvial facies (sedimentary units II to VI; 1.80 m b.s.l.) with the relative sea level that we were able to reconstruct for the western front of the navalia-temple complex (0.64 m b.s.l.), the maximum water depth at the western front of the building in the immediate transition to the harbour basin can be reconstructed as approximately 1.2 m. This is deep enough to ensure landing of smaller flat-keeled harbour boats as suggested by Heinzelmann (2020). However, one has to assume that – to ensure usability of the building complex – dredging was constantly required. The age interval found as time of use for the navalia-temple complex – the first to fourth century AD – thus represents the last period of use after the last cleaning measure was realized. Especially after abundant coarse-grained material including coarse sand and gravel (stratigraphic unit VI) has clogged chamber W4, most probably by a strong flood event of the river, re-dredging would have been necessary.

We know from both sondage 21 and core OST 7A that at that time, the harbour was hit by an extreme event from the seaside. At least two water pulses hit the harbour as documented by stratigraphic units VII and VIII leaving almost 50 cm of sand-dominated event deposits. Coin Mf 21–2 that was found in layer 2105 of sondage 21 yields a neat *terminus ad* or *post quem* for the deposition of the EWE-related layers 2103, 2117, and 2104 that correspond to stratigraphic units VII and VIII in core OST 7A, namely, AD 355–363. The processes that caused the deposition of layer 2103 itself first partly eroded the former surfaces 2105 and 2106 that are interpreted by Heinzelmann (2020) as last phase of use of the building. Further coins found in layer 2103 support this dating approach although most of the coins are considerably older and thus are considered redeposited. The youngest coin found in layer 2103 dates to AD 330–335 and is thus convincingly close the *terminus ad* or *post quem* for the EWE given with AD 355–363.

Based on this, we conclude that the building came finally out of use at or after AD 355–363 when a strong inundation event from the seaside hit the harbour area and left half a meter of sediments (Figs. 6, 10, 11, 12).

Our results, based on geoarchaeological and archaeological evidence, are in contrast to what was published by other authors.

According to Goiran et al. (2012: 6), the western river harbour at Ostia was abandoned between the first century BC and the first century AD due to siltation with sand. These authors suggested that the harbour was abandoned before the new harbour complex at Portus was founded in the midst first century AD (Goiran et al. 2014, 2017; Salomon et al. 2017). In the light of our new results documenting that both harbour and building were used until the second half of the fourth century AD, this statement cannot be longer maintained.

Goiran et al. (2014: 389; see also Delile et al. 2018: 185) further assumed that the water column in the ancient harbour basin of Ostia was less than 50 cm at the beginning of the firstst century AD due to massive siltation by the Tiber River. They also suggest a more or less precise date for the abandonment of the harbour, namely, between the first century BC and the first century AD due to siltation with sand, at the latest around 25 AD. Both the maximum water depth and the time of abandonment are not confirmed by our data. The dilemma that the navalia-temple complex was built in the Early Imperial Period is solved by Goiran et al. (2014) in that they assume that, from that time onwards, the western fluvial harbour basin was not actively used and that, during the first century AD, the Romans were unable to maintain permanent access to this harbour (Goiran et al. 2014: 395). In contrast, we can show that the construction of the navalia-temple complex in the second quarter of the first century AD goes hand in hand with the intense use of the harbour as river harbour for flat-keeled ships.

Salomon et al. (2017: 10, 11; see also Goiran et al. 2017: 80) hypothesise that, in the first century AD, large ships had to be moored offshore and river boats such as lighters were used to take the cargo upriver to Rome. Compared to the first generation lagoon-type harbour identified in the harbour basin west of Ostia (Hadler et al. 2015; Vött et al. 2015), for which water depths up to 4–5 m were determined which allowed also large ships to enter this harbour, this scenario seems plausible. The water depths being reduced now to maximum 1.20 m (Figs. 12), only flat-bottomed boats had access to the harbour and the navalia (see above). However, our data show that such an access was guaranteed until the fourth century AD, i.e., some 300 years longer than presumed by Salomon et al. (2017). The suggested definitive end of Ostia's western river harbour basin has thus to be shifted from the first century AD (Salomon et al. 2017: 19, 2018: 266; Goiran et al. 2017: 81) to the fourth century AD according to the data presented in this paper.

Goiran et al. (2017: 81), based on core data from the central harbour, are even more detailed saying that Ostia's harbour basin was no longer accessible between AD 80 and AD 230 because the maximum water depth was only 0.5 m. This

statement can now be corrected by evidence from the immediate front of the navalia-temple complex presented in this paper. Both the harbour and the navalia were accessible until the fourth century AD and ensured maximum water depth of ca. 1.2 m. However, so far, it cannot be determined precisely to what extent the former lagoonal harbour basin was used as river harbour. It may be speculated that only a considerably smaller area was continuously kept navigable for lighters in order to ensure accessibility of the navalia.

The role of high-energy events as evidenced by the sedimentary record in Ostia's western river harbour

Both stratigraphies of vibracores OST 6 and OST 7A as well as archaeological strata described from sondage 21 (Heinzelmann 2020; see Fig. 11) yield evidence of an extreme wave event (EWE) that hit Ostia's western harbour at or right after AD 355–363. From microfossil data presented in Fig. 10 and described above it is clear that the origin of this event was in the west, namely in the Tyrrhenian Sea. Similar event layers out of ex situ-allochthonous marine and/or littoral deposits of different ages were already described for Ostia's western river harbour (Hadler et al. 2015) and, most recently, also for the Fiume Morto area river harbour to the central-north of ancient Ostia (Hadler et al. 2019). The funnel-shaped river mouth of the Tiber and the overall bathymetric and coastline setting thus seems to be favourable for marine water intrusion related to EWE. Regarding the discussion whether the EWE that caused the accumulation of high-energy sediment layers as described from Ostia are storms or tsunamis, we refer to Hadler et al. (2015, 2019) who presented detailed arguments in favour of assuming tsunami dynamics for several EWE impacts that had hit the site during history. The counter argumentation for Ostia, for example, by Delile et al. (2018: 185ff.), focuses on geochemical aspects and does neither consider sedimentological nor microfossil evidence as brought forward by other authors (Hadler et al. 2015; Wunderlich et al. 2018). Similar sedimentological and microfossil evidence in favour of tsunami impact was recently published for Ostia's Fiume Morto river harbour (Hadler et al. 2019), and is now also generally confirmed for the navalia complex (this paper). An overall assumption by Marriner et al. (2017) that most of the tsunami signatures found in geological archives of the eastern Mediterranean are misinterpreted and rather represent climatic signals of increased storm activity was found to be based on incorrect statistical data treatment and rebutted by Vött et al. (2019).

However, catalogues listing historic storm, earthquake, and tsunami events are known to be incomplete (Hadler et al. 2012; Vött et al. 2019). Even if there are historic reports, their translation and interpretation remain a matter of debate. For instance, Tuck (2019) discusses whether or not the *tempestas* in AD 62 reported by Tacitus, during which 200 ships were destroyed in Ostia's harbour, was actually a tsunami. We are also convinced that storms in the Tyrrhenian Sea would not be able to produce a 0.5 m sand sheet in the former western harbour, that was deposited at least several hundreds of meters to almost 1 km inland of the river mouth at that time compared to the location of Roman villae at the strandline of these days (Bicket et al. 2009). The flood of AD 371, for example, caused several days of complete stillwater inundation in the city of Rome due to excessive rainfall (Ammianus Marcellinus: Rerum Gestarum 29.6.17–18; Aldrete 2007, Table A.1). However, this flood, after the waters had finally disappeared, left the city almost untouched and the river course unchanged. It was certainly not able to accumulate such purely marine deposits in the western harbour of Ostia as found in sediment cores and archaeological sondages. Also, harbours were designed to withstand strong storms whereas tsunami waves, on the contrary, are known to become destructively amplified in harbour basins (Röbke and Vött 2017, Tuck 2019: 442). Finally, EWE-related sediments encountered in the Ostia's western river harbour (units VII and VIII in core OST 7A) were deposited considerably above the relative sea level at the time when the harbour complex was in use (Figs. 10 and 12). Apart from this, there is no historic information on extraordinary, high-energy floods that affected the Tiber River mouth during the fourth century AD related to storm events (Camuffo and Enzi 1995; Alessandroni and Remedia 2002). All these observations speak for extraordinary depositional circumstances as known for tsunamis.

A *terminus ad* or *post quem* for the EWE that hit Ostia's western river harbour can be reliably determined as AD 355–363 based on radiocarbon ages and coin findings. Local to regional catalogues do not yield any information on local to regional-sourced earthquakes or seawaves (Guidoboni et al. 1994; Ambraseys 2009) for this time. The chronological proximity with the well-known AD 365 Crete earthquake and tsunami that affected large parts of the Mediterranean from the Levante to southern Italy may, however, be regarded more than potentially accidental.

The 21 July AD 365 event was probably triggered by a fault offshore western Crete (Shaw et al. 2008, Shaw 2012, Mouslopoulou et al. 2015). The associated tsunami devastated coasts and man-made coastal infrastructure between the Levante and Italy as documented by geological evidence (e.g. De Martini et al. 2010, 2011, Gerardi et al. 2012, Smedile et al. 2011, 2012, May et al. 2012, Ntageretzis et al. 2015, Polonia et al. 2013, 2016, Finkler et al. 2018). Impacted regions are located up to 500–600 km distant from the suggested tsunamigenic fault. Also, there are reliable historic accounts on the effects of the AD 365 tsunami on many Mediterranean coasts (Guidoboni et al. 1994; Kelly 2004; Ambraseys 2009). The idea that the AD 365 tsunami wave might have affected the Tyrrhenian Sea seems unrealistic

because of potential dissipation forces in the comparatively shallow waters between Sicily and the Tunisian coast. However, funnelling and acceleration effects maycause increased flow velocities and wave heights so that dissipation might be more than equalized. Additional wave reflection effects along the Libyan and Tunisian coasts may induce wave redirection dynamics towards the N. Moreover, on a speculative base, several waves east of Malta, due to wave interferences, may form a single, composite large wave that may proceed to the north (see Shaw et al. 2008: Fig. 4). Thus, on a merely hypothetical base, a tele-tsunami wave caused by the AD 365 event could have reached the central Tyrrhenian Sea. Event-related secondary events such as underwater slides along the north African shelves may also be considered as tsunamigenic processes.

Hadler et al. (2015, 2019) found sedimentary and chronological evidence of older tsunami impacts on Ostia's harbours – both to the west of the city and along the Fiume Morto channel –, namely, for the fourth to second century BC and the time right before the construction of the navalia-temple complex in the fistst century AD. Traces of the event that occurred at or shortly after AD 355–363 are only known for the navalia-temple area (this paper). One may assume that this tsunami also affected areas further landward and tsunami sediments were transported eastward along the Tiber River and deposited in the Fiume Morto channel. Possibly, these deposits were eroded by a younger river channel that was deeply incised down to ca. 8 m b.s.l. during early medieval times (Hadler et al. 2019: Fig. 13).

Beyond this theoretical discussion, there is archaeoseismological evidence of a strong seismic event that hit Sicily in AD 365 and historic accounts that document the occurrence of a related tsunami (Bottari et al. 2009: 168–170, see also Stiros 2001). Whether or not this may have something to do with the AD 365 Crete event or is related to regional events, has to be clarified by future investigations.

Conclusions

We conducted detailed geoarchaeological investigations at the immediate western front of the navalia-temple complex in Ostia's western harbour. Results were compared with archaeological data obtained from excavations accomplished in 2000/2001 and published by Heinzelmann (2020). A multiproxy approach was used to reconstruct the history and evolution of Ostia's western river harbour. The main conclusions can be summarized as follows:

(1) Based on ERT studies along the western front of the navalia-temple-complex, it was possible to identify subsurface structures and evaluate the local stratigraphy. ERT depth sections were used to determine vibracoring sites.
(2) Rectangular-shaped resistivity anomalies were investigated by vibracoing. Core OST 6 was drilled through an anomaly with low resistivity values and brought to light a more than 1 m thick section of an *opus reticulatum* wall with parts of the original *opus latericium* on top. Core OST 7A was drilled in an anomaly with higher resistivity values that turned out to be the sedimentary infill of a formerly vaulted chamber of the navalia-temple complex. Comparing ERT data and stratigraphic results with archaeological information results in the diagnosis that core OST 6 hit the wall between chambers W4 and W5 according to Heinzelmann (2020).
(3) The sedimentary sequence recorded in core OST 7A comprises nine different stratigraphic units from basal pre-harbour lagoonal deposits (unit I) to fluvial

Fig. 13 Visualization of a reconstruction scenario for the navalia-temple complex at ancient Ostia for the first to fourth century AD. The vaulted chambers in the substruction of the temple terrace exposed to the west are accessible from the river harbour basin. In this scenario, the northern chambers are not used as navalia. Source: Heinzelmann (2020). For further details, see text and Heinzelmann (2020)

sediments associated with the harbour in use (units II to VI), deposits of an extreme wave event from the seaside (units VII and VIII) to alluvial deposits (unit IX).

(4) Based on radiocarbon dating, the navalia were in use between the first and the fourth century AD with a water depth of maximum ca. 1.2 m at the immediate western front of the building. The age is in agreement with the date of construction of the navalia-temple complex in the second quarter of the first century AD (Heinzelmann and Martin 2002). The relative sea level at that time was reconstructed to be around 0.64 m b.s.l. The harbour and the navalia were obviously accessible only for flat-keeled leighters, cargo boats, and river warships. Larger cargo ships that were able to access the 1st generation lagoonal harbour at this site between the second and fourth century BC (Hadler et al. 2015; Vött et al. 2015) could no longer be directly unloaded in this harbour and were probably moored offshore, their freight being reloaded to the mentioned leighters.

(5) Based on geoarchaeological and archaeological chronostratigraphic data, the navalia-temple complex was in use until the second half of the fourth century AD. It was not before AD 355–363 or shortly afterwards, that the harbour site was abandoned. Ostia's harbour was neither abandoned nor completely silted up before the harbour at Portus was established as previously assumed by other authors.

(6) The western front of the navalia-temple complex was hit by an extreme wave event, leaving a sand layer approx. 0.5 m thick, at or shortly after AD 355–363 which led to the final abandonment of Ostia's river harbour. Based on sedimentary, geochemical, and microfaunal data and evaluated against potential storm influence, this event is interpreted as a tsunami that hit the wider coastal region.

Acknowledgments Thanks are due to P. Germoni and M. Barbera from the Soprintendenza Speciale per i Beni Archeologici di Roma of the Ministero dei Beni e delle Attività Culturali e del Tourismo for work permits. We are also grateful to Archer Martin for his valuable contribution to the discussion of the results. We finally acknowledge funding of the project 'The River Harbour of Ostia' by the German Research Foundation (VO 938/10-1, HE 3680/6-1) within the Priority Programme 1630 'Harbours from the Roman Period to the Middle Ages'.

Funding Information Open Access funding provided by Projekt DEAL.

References

Aldrete GA (2007) Floods of the Tiber in ancient Rome. The Johns Hopkins University Press, Baltimore 338 pp

Alessandroni MG, Remedia G (2002) The most severe floods of the Tiber River in Rome. In: International Association of Hydrological Scientists (eds., IAHS) the extreme of the extremes: extraordinary floods. Proceedings internat. Symposium, Reykjavik, Iceland, 2000. IAHS publication 271: 129–132

Ambraseys N (2009) Earthquakes in the Mediterranean and Middle East. A multidisciplinary study of seismicity up to 1900. Cambridge University press, Cambridge 947 pp

Barsch H, Billwitz K, Bork H-R (Eds., 2000) Arbeitsmethoden in Physiogeographie und Geoökologie. Stuttgart, 612 pp

Bicket AR, Rendell HM, Claridge A, Rose P, Andrews J, Brown FSJ (2009) A multiscale geoarchaeological approach from the Laurentine shore (Castelporziano, Lazio, Italy). Géomorphologie: Relief, Processus, Environ 4:257–270 https://geomorphologie.revues.org/7720

Blackman D, Rankov B, Baika K, Gerding H, Pakkanen J (2014) Shipsheds of the ancient Mediterranean. Cambridge University Press, Cambridge 614 pp

Bottari C, Stiros SC, Teramo A (2009) Archaeological evidence for destructive earthquakes in Sicily between 400 B.C. and a.D. 600. Geoarchaeology 24(2):147–175

Calza G, Becatti G, Gismondi I, Bloch H (1953) Scavi di Ostia I. Topografia Generale, Roma

Camuffo D, Enzi S (1995) The analysis of two bi-millennial series: Tiber and Po river floods. In: Jones PD, Bradle RS, Jouzel J (eds.) Climatic variations and forcing mechanisms of the last 2000 years. NATO ASI Series, Series I: Global Environmental Change 41:433–450

Cimerman F, Langer MR (1991) Mediterranean Foraminifera. Academia Scientiarum et Artium Slovenica Classis IV: Historia Naturalis 30: 1–119

Coarelli F (1997) Il Campo Marzio: dalle origini alla fine della repubblica. Quasar, Roma 676 pp

De Martini PM, Barbano MS, Smedile A, Gerardi F, Pantosti D, Del Carlo P, Pirrotta C (2010) A unique 4000 year long geological record of multiple tsunami inundations in the Augusta bay (eastern Sicily, Italy). Mar Geol 276:42–57

De Martini PM, Barbano MS, Pantosti D, Smedile A, Pirrotta C, Del Carlo P, Pinzi S (2012) Geological evidence for paleotsunamis anlong eastern Sicily (Italy): an overview. Natura Hazards and Earth System Sciences 12:2569–2580

Delile H, Goiran J-P, Blichert-Toft J (2018) The contribution of geochemistry to ancient harbor geoarchaeology: the example of Ostia Antica. Quat Sci Rev 193:170–187

Donato SV, Reinhardt EG, Boyce JI, Rothaus R, Vosmer T (2008) Identifying tsunami deposits using bivalve shell taphonomy. Geology 36(3):199–202

Ferkel H, Konen H, Schäfer C (2004) Navis lusoria. Ein Römerschiff in Regensburg. St. Katharinen Scripta Mercaturae Verlag, Regensburg 144 pp

Finkler C, Fischer P, Baika K, Rigakou D, Metallinou G, Hadler H, Vött A (2018) Tracing the Alkinoos Harbor of ancient Kerkyra, Greece, and reconstructing its paleotsunami history. Geoarchaeology 33(1): 24–42. https://doi.org/10.1002/gea.21609

Fischer P, Wunderlich T, Rabbel W, Vött A, Willershäuser T, Baika K, Rigakou D, Metallinou G (2016) Combined electrical resistivity tomography (ERT), direct-push electrical conductivity logging

(DP-EC) and coring – a new methodological approach in geoarchaeological research. Archaeological Prospection 23/3:213–228. https://doi.org/10.1002/arp.1542

Gerardi F, Smedile A, Pirrotta C, Barbano MS, De Martini PM, Pinzi S, Gueli AM, Ristuccia GM, Stella G, Troja O (2012) Geological record of tsunami inundations in Pantano Morghella (South-Eastern Sicily) both from near- and far-field sources. Nat Hazards Earth Syst Sci 12:1185–1200. https://doi.org/10.5194/nhess-12-1185-2012

Goiran J-P (2012) The first harbour of ancient Rome rediscovered. CNRS press release, 7 décembre 2012. https://www2.cnrs.fr/en/2143.htm

Goiran J-P, Tronchère H, Salomon F, Carbonel P, Djerbi H, Ognard C (2010) Palaeoenvironmental reconstruction of the ancient harbors of Rome: Claudius and Trajan's marine harbors on the Tiber delta. Quarter Int 216:3–13. https://doi.org/10.1016/j.quaint.2009.10.030

Goiran J-P, Salomon F, Pleuger E, Vittori C, Mazzini I, Boetto G, Arnaud P, Pellegrino A (2012) Port antique d'ostie. Résultats preliminaires de la première champagne de carottages. Chronique des activités archeologiques de l'École française de Rome, Italie central, mis en ligne le 19 décembre 2012. https://cefr.revues.org/299

Goiran J-P, Salomon F, Mazzini I, Bravard J-P, Pleuger E, Vittori C, Boetto G, Christiansen J, Arnaud P, Pellegrino A, Pepe C, Sadori L (2014) Geoarchaeology confirms location of the ancient harbour basin of Ostia (Italy). J Archaeol Sci 41:389–398. https://doi.org/10.1016/j.jas.2013.08.019

Goiran J-P, Salomon F, Vittori C, Delile H, Christiansen J, Oberlin C, Boetto G, Arnaud P, Mazzini I, Sadori L, Poccardi G, Pellegrino A (2017) High chrono-stratigraphical resolution of the harbour sequence of Ostia: palaeo-depth of the basin, ship draught and dredging. In: Franconi V (ed.) fluvial landscapes in the Roman world. J Roman Archaeol Suppl Series 104:68–84

Guidoboni E, Comastri A, Traina G (1994) Catalogue of ancient earthquakes in the Mediterranean area up to the 10th century. Volume 1. Bologna, ING-SGA 504 pp

Hadler H, Willershäuser T, Ntageretzis K, Henning P, Vött A (2012) Catalogue entries and non-entries of earthquake and tsunami events in the Ionian Sea and the Gulf of Corinth (eastern Mediterranean, Greece) and their interpretation with regard to palaeotsunami research. In: Vött A, Venzke J-F (eds.) Beiträge der 29. Jahrestagung des Arbeitskreises „Geographie der Meere und Küsten", 28.-30. April 2011, Bremen. Bremer Beiträge zur Geographie und Raumplanung 44: 1–15. https://elib.suub.uni-bremen.de/edocs/00102756-1.pdf

Hadler H, Vött A, Fischer P, Ludwig S, Heinzelmann M, Rohn C (2015) Temple-complex post-dates tsunami deposits found in the ancient harbour basin of Ostia (Rome, Italy). J Archaeol Sci 61:78–89 https://doi.org/10.1016/j.jas.2015.05.002

Hadler H, Fischer P, Obrocki L, Heinzelmann M, Vött A (2019) River channel evolution and tsunami impacts recorded in local sedimentary archives – the 'Fiume Morto' at Ostia Antica (Tiber River, Italy). Sedimentology 1-35. https://doi.org/10.1111/sed.12599

Heinzelmann M (1998) Arbeitsbericht zu einer zweiten geophysikalischen Prospektionskampagne in Ostia. Römische Mitteilungen 105:425–429

Heinzelmann M (2001) Ostia. Vorbericht zur dritten Grabungskampagne 2000. Römische Mitteilungen 108:313–325

Heinzelmann M (2010) Supplier of Rome or Mediterranean marketplace? The changing economic role of Ostia after the construction of Portus in the light of new archaeological evidence. Bolletino di Archeologia on line I 2010, volume speciale B/B7/2

Heinzelmann M (2020) Forma Urbis Ostia 1. Ergebnisse der stratigraphischen Untersuchungen in den unausgegrabenen Stadtgebieten. Reichert-Verlag, Wiesbaden (in press)

Heinzelmann M, Martin A (2002) River port, navalia and a harbour temple at Ostia – new results of a joint DAI-AAR project. J Roman Archaeol 15:5–19

Keay S, Millett M, Paroli L, Strutt K (2005) Portus. An archaeological survey of the port of the Imperial Rome. Archaeological monographs of the British School at Rome 15, London. 360 pp.

Kelly G (2004) Ammianus and the great tsunami. J Roman Stud 94:141–167

Köhn M (1929) Korngrößenbestimmung vermittels Pipettanalyse. Tonindustrie-Zeitung 55:729–731

Lanciani R (1868) Ricercher topografiche sulla città die Porto. AdI 40: 144–195

Loeblich AR, Tappan HN (1988) Foraminiferal genera and their classification. Springer US, New York 970 pp

Marriner N, Kaniewski D, Morhange C, Flaux C, Giaime M, Vacchi M, Goff J (2017) Tsunamis in the geological record: Making waves with a cautionary tale from the Mediterranean. Sci Adv 3/10: 31700485. https://doi.org/10.1126/sciadv.1700485

Martin A, Heinzelmann M, De Sena EC, Granino Cecere MG (2002) The urbanistic project on the previously unexcavated areas of Ostia (DAI-AAR 1996-2001). Memoirs Am Acad Rome 47:259–304

May SM, Vött A, Brückner H, Smedile A (2012) The Gyra washover fan in the Lefkada lagoon, NW Greece – possible evidence of the 365 AD Crete earthquake and tsunami. Earth, Planets Space 64:859–874. https://doi.org/10.5047/eps.2012.03.007

Meiggs R (1973) Roman Ostia. Clarendon Press, University of California 622 pp

Mischke S, Schudack U, Bertrand S, Leroy SAG (2012) Ostracods from a Marmara Sea lagoon (Turkey) as tsunami indicators. Quat Int 261: 156–161

Mouslopoulou V, Nicol A, Begg J, Oncken O, Moreno M (2015) Clusters of megaearthquakes on upper plate faults control the Eastern Mediterranean hazard. Geophysical Research Letters 42. https://doi.org/10.1002/2015GL066371

Murray JW (2006) Ecology and applications of benthic foraminifers. Cambridge University Press, Cambridge 426 pp

Ntageretzis K, Vött A, Emde K, Fischer P, Hadler H, Röbke BR, Willershäuser T (2015) Palaeotsunami record in near-coast sedimentary archives in southeastern Lakonia (Peloponnese, Greece). Zeitschrift für Geomorphologie N.F Suppl Issue 59(4):275–299. https://doi.org/10.1127/zfg_suppl/2015/S-00208

Obrocki L, Vött A, Wilken D, Fischer P, Willershäuser T, Koster B, Lang F, Papanikolaou I, Rabbel W, Reicherter K (2019) Tracing tsunami signatures of the AD 551 and AD 1303 tsunamis at the Gulf of Kyparissia (Peloponnese, Greece) using Direct Push in situ sensing techniques combined with geophysical studies. Sedimentology https://doi.org/10.1111/sed.12555

Paschetto L (1912) Ostia, Colonia Romana. Roma

Pilarczyk JE, Dura T, Horton BP, Engelhart SE, Kemp AC, Sawai Y (2014) Microfossils from coastal environments as indicators of paleo-earthquakes, tsunamis and storms. Palaeogeogr Palaeoclimatol Palaeoecol 413:144–157. https://doi.org/10.1016/j.palaeo.2014.06.033

Polonia A, Bonatti E, Camerlenghi A, Lucchi RG, Panieri G, Gasperini L (2013) Mediterranean megaturbidite treiggered by the AD 365 Crete earthquake and tsunami. Sci Rep 3:1285

Polonia A, Vaiani SC, de Lange GJ (2016) Did the a.D. 365. Crete earthquake/tsunami trigger synchronous giant turbidity currents in the Mediterranean Sea? Geology 44(3):191–194

Röbke BR, Vött A (2017) The tsunami phenomenon. Prog Oceanogr 159:296–322. https://doi.org/10.1016/j.pocean.2017.09.003

Salomon F, Keay S, Carayon N, Goiran J-P (2017) The development and characteristics of ancient harbours – applying the PADM chart to the case studies of Ostia and Portus. PLoS ONE 11(9):e0162587 and correction: 12 (1):e0170140. https://doi.org/10.1371/journal.pone.0170140

Salomon F, Goiran J-P, Noirot B, Pleuger E, Bukowiecki E, Mazzini I, Carbonel P, Gadhoum A, Arnaud P, Keay S, Zampini S, KAy S, Raddi M, Ghelli A, Pellegrino A, Morelli C, Germoni P (2018) Geoarchaeology of the Roman port-city of Ostia: Fluvio-coastal

mobility, urban development and resilience. Earth-Science Reviews 177:265–283. https://doi.org/10.1016/j.earscirev.2017.10.003

Sen Gupta BKS (1999) Modern Foraminifera. Kluwer Academic Publisher, Dordrecht 371 pp

Shaw B, Ambrayses NN, England PC, Floyd MA, Gorman GJ, Highham TFG, Jackson JA, Nocquet, J-M, Pain CC, Piggott MD (2008) Eastern Mediterranean tectonics and tsunami hazard inferred from the AD 365 earthquake. Nat Geosci, https://www.nature.com/doifinder/10.1038/ngeo151

Shaw B (2012) The AD 365 earthquake: Large tsunamigenic earthquakes in the Hellenic Trench. In: Shaw B: Active tectonics of the Hellenic subduction zone. Springer Theses, pp. 7-28. Springer, Berlin, Heidelberg. https://doi.org/10.1007/978-3-642-20804-1_2

Smedile A, De Martini PM, Pantosti D, Bellucci L, Del Carlo P, Gasperini L, Pirrotta C, Polonia A, Boschi E (2011) Possible tsunami signatures from an integrated study in the Augusta bay offshore (eastern Sicily – Italy). Mar Geol 281:1–13

Smedile A, Martini PM, Pantosti D (2012) Combining inland and offshore paleotsunami evidence: the Augusta bay (eastern Sicily, Italy) case study. Nat Hazards Earth Syst Sci 12:2557–2567

Stiros SC (2001) The AD 365 Crete earthquake and possible seismic clustering during the fourth to sixth centuries AD in the eastern Mediterranean: a review of historical and archaeological data. J Struct Geol 23(2–3):545–562

Stuiver M, Reimer PJ, Reimer RW (2019) CALIB 7.1 [WWW program] at https://calib.org, accessed 2019-9-10

Tuck SL (2019) Was the tempestas of AD 62 at ostia Antica actually a tsunami? Class J 114(4):439–462

Visconti CL (1857) Escavazioni di Ostia dall'anno 1855 al 1858. AdI 29: 281–340

Vött A, Fischer P, Hadler H, Ludwig S, Heinzelmann M, Rohn C, Wunderlich T, Wilken D, Erkul E, Rabbel W (2015) Detection of two different harbour generations at ancient Ostia (Italy) by means of geophysical and stratigraphical methods. In: Schmidts T, Vučetić M. (eds.) Häfen im 1. Millennium A.D. Bauliche Konzepte, herrschaftliche und religiöse Einflüsse. RGZM-Tagungen 22: 23–34 (= Interdisziplinäre Forschungen zu den Häfen von der Römischen Kaiserzeit bis zum Mittelalter, Vol. 1: 23–34, edited by von Carnap-Bornheim C, Daim F, Ettel P, Warnke U) Mainz

Vött A, Bruins HJ, Gawehn M, Goodman-Tchernov BN, De Martini PM, Kelletat D, Mastronuzzi G, Reicherter K, Röbke BR, Scheffers A, Willershäuser T, Avramidis P, Bellanova P, Costa PJM, Finkler C, Hadler H, Koster B, Lario J, Reinhardt E, Mathes-Schmidt M, Ntageretzis K, Pantosti D, Papanikolaou I, Sansò P, Scicchitano G, Smedile A, Szczuciński W (2019) Publicity waves based on manipulated geoscientific data suggesting climatic trigger for majority of tsunami findings in the Mediterranean – response to 'tsunamis in the geological record: making waves with a cautionary tale from the Mediterranean' by Marriner et al. (2017). Zeitschrift für Geomorphologie N.F. Suppl. Issue 62(2):7–45. https://doi.org/10.1127/zfg_suppl/2018/0547

Wunderlich T, Wilken D, Erkul E, Rabbel W, Vött A, Fischer P, Hadler H, Heinzelmann M (2018) The river harbour of Ostia Antica – stratigraphy, extent and harbor infrastructure from combined geophysical measurements and drillings. Quat Int 473(A):55–65. https://doi.org/10.1016/j.quaint.2017.07.017